Formin-induced actin cables are required for polarized recruitment of the Ste5 scaffold and high level activation of MAPK Fus3

Maosong Qi and Elaine A. Elion

Journal of Cell Science 120, 712 (2007) doi:10.1242/jcs03398

There was an error published in *J. Cell Sci.* **118**, 2837-2848 (2005).

Throughout the article and in the supplementary figures, the plasmid GFP-Ste5 was incorrectly referred to as Ste5-GFP.

The authors apologise for this error.

Formin-induced actin cables are required for polarized recruitment of the Ste5 scaffold and high level activation of MAPK Fus3

Maosong Qi and Elaine A. Elion*

Department of Biological Chemistry and Molecular Pharmacology, Harvard Medical School, MA 02115, USA

*Author for correspondence (e-mail: elaine_elion@hms.harvard.edu)

Accepted 5 April 2005
Journal of Cell Science 118, 2837-2848 Published by The Company of Biologists 2005
doi:10.1242/jcs.02418

Summary

Little is known about how a mitogen-activated protein kinase (MAPK) cascade is targeted to specific sites at the plasma membrane during receptor stimulation. In budding yeast, the Ste5 scaffold is recruited to a receptor-coupled G protein during mating pheromone stimulation, allowing the tethered MAPK cascade to be activated by Ste20, a Cdc42-anchored kinase. Here we show that stable recruitment of Ste5 at cortical sites requires the formin Bni1, Bni1-induced actin cables, Rho1 and Myo2. Rho1 directs recruitment of Bni1 via the Rho-binding domain, and Bni1 mediates localization of Ste5 through actin cables and Myo2, which co-immunoprecipitates with Ste5 during receptor stimulation. Bni1 is also required for polarized recruitment and full activation of MAPK Fus3, which must bind Ste5 to be activated, and polarized recruitment of Cdc24, the guanine exchange factor that binds Ste5 and promotes its recruitment to the G protein. In contrast, Bni1 is not important for activation of MAPK Kss1, which can be activated while not bound to Ste5 and does not accumulate at cortical sites. These findings reveal that Bni1 mediates the formation of a Ste5 scaffold/Fus3 MAPK signaling complex at polarized sites, and suggests that a pool of Ste5 may translocate along formin-induced actin cables to the cell cortex.

Supplementary material available online at
http://jcs.biologists.org/cgi/content/full/118/13/2837/DC1

Key words: Ste5 scaffold, MAPK, Formin, Bni1, Actin cytoskeleton, Polarization

Introduction

Eukaryotic cells frequently respond to external stimuli with signal transduction pathways that are activated by plasma membrane receptor-linked G proteins and GTPases (Leof, 2000). Often, scaffold proteins mediate the linkage of a G protein or GTPase to effectors and their targets. This general regulatory device is used by cells to respond to a wide variety of extracellular stimuli and is particularly crucial for cell polarity and migration (Palmieri and Haarer, 1998; Garrington and Johnson, 1999; Henrique and Schweisguth, 2003). Scaffold proteins play important roles in the activation of mitogen-activated protein kinase (MAPK) cascades by G proteins and GTPases and have been speculated to specify and intensify the activation of kinases and assemble them at sites of stimulation (Elion, 1995; Burack and Shaw, 2000; Garrington and Johnson, 1999; Morrison and Davis, 2003). A number of MAPK scaffolds have been identified, including Ste5, Pbs2, the JIPs (JIP-1, JIP-2, JIP3, JSAP1), KSR and β-arrestin (Elion, 1995; Morrison and Davis, 2003). MAPK scaffolds can be asymmetrically enriched at plasma membrane sites, suggesting their localization may be sensitive to spatial cues of cell polarity and they, in turn, may influence cell polarity (Mahanty et al., 1999; Kelkar et al., 2000; Muller et al., 2001; Ge et al., 2003).

Many stimuli that activate MAPK cascades also stimulate changes in cell morphology and motility through GTPase-induced changes in the actin and microtubule cytoskeletons. For example, Rho-type GTPases, including Cdc42, play a central role in mediating cell polarity by establishing asymmetry by binding a wide variety of effector proteins that nucleate actin filaments and localize microtubules at leading edges in eukaryotic cells (Erickson and Cerione, 2001). Key downstream effectors of Rho-type GTPases include WASP family proteins and formin homology (FH) proteins that nucleate higher-order actin structures (Takenawa and Miki, 2001; Zigmond, 2004). Many intersections between regulators of the actin cytoskeleton and signaling pathways also exist. For example, Cdc42 anchors p21-activated kinases (PAKs) that directly phosphorylate mitogen-activated protein kinase kinase kinase (MAPKKKs) (Bokoch, 2003), and binds to the Par6-Par3 complex and activates atypical protein kinase C (Etienne-Manneville and Hall, 2003). In mammalian T cells, the actin cytoskeleton may function as a scaffold for signaling components such as PKC-θ (Dustin and Cooper, 2000). The complexity of these interactions makes it difficult to establish the order of events.

The response to mating pheromone in budding yeast provides a system to study the relationship between signal transduction and the actin cytoskeleton. Cells respond to mating pheromone through a MAPK cascade that is activated by a serpentine receptor coupled to a heterotrimeric G protein, which releases an inhibitory Gα subunit from a stimulatory βγ

dimer (Ste4/Ste18; Fig. 1A) (Dohlman and Thorner, 2001; Bardwell, 2004). Two MAPKs are activated, Fus3 and Kss1, however, Fus3 is the crucial kinase for cell cycle arrest, polarized morphological changes associated with mating differentiation and cell fusion to form a zygote (Elion et al., 1990; Elion et al., 1991; Farley et al., 1999). MAPK activation triggers transcriptional activation of many genes, cell cycle arrest in G1 phase and polarized growth, resulting in a pear-shaped cell or shmoo. The polarized growth is chemotropic and involves localized enrichment of the receptor and G protein at sites of growth (Arkowitz, 1999). The Ste5 scaffold plays an essential role in these events by binding to the G protein β subunit (Ste4) and a MAPK cascade consisting of Ste11 (MAPKKK), Ste7 (MAPKK) and Fus3 (MAPK) (Elion, 2001). Pathway activation occurs through juxtaposition of the Ste5-multikinase complex with Ste20, a p21-activated kinase (PAK) that is anchored to Cdc42 at the plasma membrane and directly phosphorylates Ste11. Fus3 must bind to Ste5 to be activated, whereas Kss1 is activated from the Ste5 scaffold (Andersson et al., 2004). Once activated, it is thought that Fus3 is released from the scaffold complex to phosphorylate targets throughout the cell.

Cell polarity during pheromone signaling is dependent on the actin cytoskeleton. Optimal pathway activation requires a number of regulators of the cytoskeleton apart from Cdc42 and Ste20, including the Cdc42 guanine exchange factor Cdc24 (Zhao et al., 1995) and Bem1 (Lyons et al., 1996). The addition of latrunculin A to pheromone-treated cells blocks polarized recruitment of a number of cell polarity proteins including Cdc42, Rho1 and Bem1 and reduced expression of a pathway reporter gene (Ayscough and Drubin, 1998). These findings suggest that polarized recruitment of these factors by the actin cytoskeleton could play a role in MAPK activation.

The localization of the Ste5 scaffold at the cell cortex is also polarized and requires prior nuclear shuttling, which is also required for activation of Fus3 (Mahanty et al., 1999). In the absence of pheromone, a small pool of Ste5 accumulates at cortical sites in G2/M and G1 phase cells through a process that involves Cdc42, Cdc24 and Bem1, and is independent of Ste4 and the actin cytoskeleton (Wang et al., 2005). Cdc24 shuttles through the nucleus (Gulli and Peter, 2001), binds to Ste5 and promotes nuclear accumulation and recruitment of Ste5 (Wang et al., 2005). These, and other findings, suggest that Ste5 is basally recruited by internal cues set up by Bem1, Cdc42 and Cdc24, which may shuttle through the nucleus and be recruited with Ste5 as a complex. During pheromone stimulation, polarized recruitment of Ste5 becomes dependent upon the actin cytoskeleton in addition to Ste4 (Wang et al., 2005). Ste5 is detected at the cortex of G1 phase cells within minutes after α factor addition and is found at the tips of emerging shmoos (Pyciak and Huntress, 1998; Mahanty et al., 1999). Fus3 also localizes at the shmoo tip, but fluorescence recovery after photobleaching (FRAP) analysis suggests its residency has a much shorter half-life than that of Ste5 (van Drogen et al., 2001). Here, we show that during pheromone stimulation, the formin Bni1 is essential for Ste5 scaffold recruitment at cortical sites and controls Ste5 recruitment through actin cables. Bni1 is also required for cortical recruitment of Cdc24, efficient activation of Fus3 and stable recruitment of Fus3 at the cell cortex. Myo2 is required for cortical localization of Ste5 and is found in Ste5 immune complexes during pheromone-stimulation, raising the possibility that a pool of Ste5 may translocate along actin cables via Myo2.

Materials and Methods

Yeast strains and plasmid construction

Details can be found in supplementary material.

Quantitative mating and pheromone response assays

Mating assays were performed as described previously (Sprague, 1991). The percentages of unbudded and shmooed cells were quantitated after a 2-hour exposure to 50 nM α factor. *FUS1* transcription was assayed with a *FUS1-lacZ* reporter gene maintained in a 2μ plasmid. β-galactosidase activity was quantitated as described previously (Lyons et al., 1996). Halo assays were performed as described previously (Lyons et al., 1996) using 5 μl of 2 mM or 0.1 mM α factor in dimethylsulfoxide, depending on whether strains were *SST1* or *sst1*. *ste5Δ* is a null allele of *STE5*.

Yeast whole cell extracts and MAPK activation assay

Yeast strains were grown at 30°C in selective SC medium containing 2% dextrose to an A_{600} of ~0.6. Cells were treated with α factor or induced with 2% galactose. Whole cell extracts (WCE) were prepared as described previously (Elion et al., 1993) except that the modified H buffer contains 250 mM NaCl. Protein concentrations were determined with the Bio-Rad protein assay. Fus3 kinase assays were done as described previously (Elion et al., 1993). To detect MAPK phosphorylation, 200 μg total protein was separated by 10% SDS-PAGE, then transferred onto a nitrocellulose membrane (Schleicher and Schuell, Keene, NH, USA). The membrane was blocked with 5% skim milk in Tris-buffered saline (TBS) containing 0.1% Tween 20, then in the same buffer containing rabbit anti-phospho-p44/p42 antibody (1:1000; Cell Signaling, Beverly, MA, USA), followed by washing and incubation in the same buffer containing horseradish peroxidase-coupled goat anti-rabbit antibody (1:10000, Bio-Rad). After the signal was visualized with ECL (Amersham), the membrane was stripped and reprobed with anti-Tcm1 monoclonal antibody (from J. Warner, Albert Einstein College of Medicine, Bronx, NY).

Immunoprecipitation

One mg of WCE was mixed with 3 μg 12CA5 antibody (ascites provided by Harvard University antibody facility) in modified H buffer with 150 mM NaCl and incubated on ice for 45 minutes. 50 μl protein A-Sepharose beads (Pharmacia) were added and samples were rotated at 4°C for 2 hours. The beads were washed three times with modified H buffer and then boiled in protein loading buffer. Samples were separated with 8% SDS-PAGE and transferred onto nitrocellulose membrane. The membrane was then probed with 9E10 (ascites from Harvard University antibody facility) or 12CA5 monoclonal antibody.

Visualization of Ste5-Myc9 and GFP-tagged protein localization

Ste5, Ste20, Cdc24, Fus3 and Bni1 tagged with GFP were observed with direct fluorescence. Cells were treated with α factor then fixed in 3.7% formaldehyde for 45 minutes. After washing with PBS and brief sonification, cells were mounted in Vectashield medium (Vector Laboratories). Ste5 tagged with Myc9 was visualized by indirect immunofluorescence as described previously (Mahanty et al., 1999) with some modifications. Cells were fixed with 3.7% formaldehyde for 45 minutes at room temperature, spheroplasted for 30 minutes in

PBS containing 100 μg/ml lyticase, 3 μg/ml phenylmethylsulphonyl fluoride and 2 μl/ml β-mercaptoethanol. Cells were then fixed in –20°C methanol for 5 minutes followed by 20 seconds in –20°C acetone. After being air-dried, cells were permeabilized with 0.5% Triton X-100 for 5 minutes, washed with PBS three times, and then blocked with 2% BSA at room temperature for 1 hour. To detect Myc-tagged Ste5, samples were incubated in a 1:1000 dilution of 9E10 ascites fluid at room temperature for 1 hour or at 4°C overnight. After washing with PBS, samples were exposed to a CY3-conjugated secondary antibody (1:1000, Zymed Laboratories, South San Francisco, CA, USA) and incubated in the dark for 1 hour. After four washes with PBS, the slides were mounted with Vectashield medium. All samples were observed on an Axioskop 2 microscope (Carl Zeiss, Thornwood, NY, USA) linked to a digital camera (C4742-95; Hamamatsu, Bridgewater, NJ, USA).

Temperature shift experiments, latrunculin A treatment and actin staining

Cells were grown at room temperature then shifted to the nonpermissive temperature as follows: *bni1*^{TS}*bnr1Δ* and *tpm1*^{TS} *tpm2Δ* cells were shifted to media that were pre-warmed to 34°C and 34.5°C, respectively, and 5 μM α factor was added to the culture at the same time. Cells were incubated at the nonpermissive temperature for 10 minutes, then fixed for immunostaining. *rho1-2* and *rho1-104* cells were first shifted to 37°C for 1 hour before being treated with 5 μM α factor for 30 minutes and *myo2-66* cells were pre-cultured at 37°C for 2 hours, then both were stimulated with 5 μM α factor for 30 minutes before being fixed. Strains harboring *GAL1-MYO2DN* were grown in 2% galactose for 1 hour and then incubated with 5 μM α factor for 15 minutes.

Latrunculin A (Molecular Probes) was dissolved in dimethylsulfoxide (DMSO) at 5 mM and the stock solution was stored at –20°C. To treat the cells, latrunculin A was added to the medium at a final concentration of 100 μM and DMSO was used as control.

To visualize actin, cells were fixed with 4% formaldehyde for 45 minutes and then stained with Rhodamine-phalloidin (Molecular Probes; final concentration 5 U/ml) in the dark for 1 hour. Cells were washed twice in PBS and resuspended in Vectashield mounting medium. Actin was examined using a Axioskop 2 microscope.

Results

Bni1 is required for efficient pheromone-induced MAPK activation

We identified *BNI1* in a targeted screen for cytoskeletal and cell polarity genes required for efficient G1 arrest induced by α mating pheromone (C.M. and E.E., unpublished). Although Bni1 was known to be required for mating pheromone-induced actin reorganization and cell polarization, it has not been thought to play a direct role in signal transduction (Evangelista et al., 1997; Buehrer and Errede, 1997). Since G1 arrest requires the activation of MAPK Fus3, we investigated a possible relationship between actin cytoskeleton reorganization by Bni1 and MAPK signal transduction. We used a previously published *bni1* null mutant in the W303-1a background (Evangelista et al., 1997) in which mating pathway functions are strictly dependent upon the MAPKs Fus3 and Kss1 (Elion et al., 1991). The *bni1Δ* mutant was severely defective in α factor-induced shmoo formation (Fig. 1B) and mated at reduced frequency (Fig. 1D) as previously shown. In addition, the strain also underwent less efficient G1 arrest in a halo assay (Fig. 1C), accumulated fewer unbudded cells after treatment with α factor (Fig. 1D) and expressed a *FUS1-lacZ* reporter gene for the pathway less efficiently than the WT strain (Fig. 1E). We note that the previous analysis of a

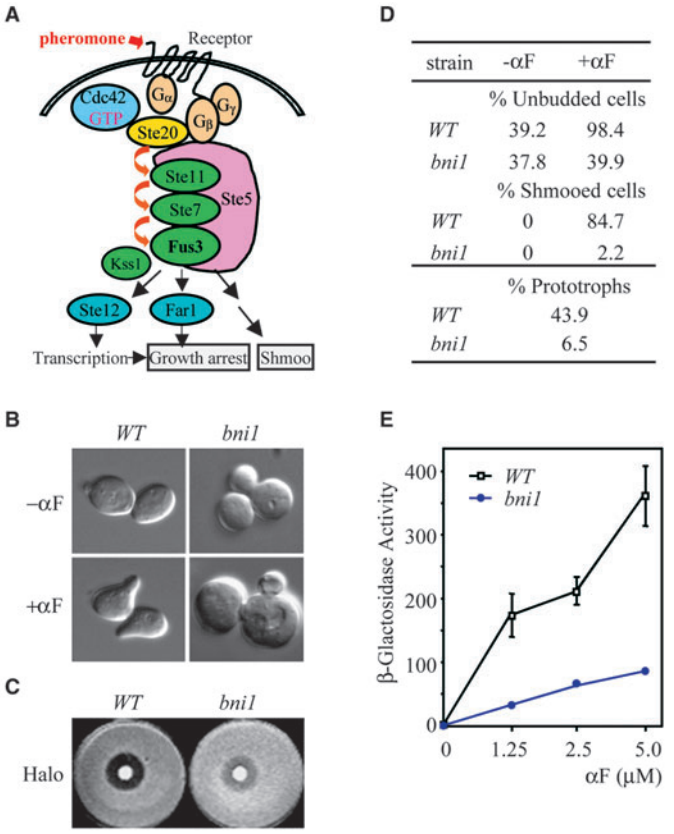

Fig. 1. *bni1Δ* mutant cells are defective in mating pathway responses. (A) Schematic diagram of yeast mating MAPK pathway. Binding of mating pheromone (α factor) to its seven-transmembrane receptor (Ste2) induces dissociation of a heterotrimeric G protein, creating free Gβγ (Ste4/Ste18) dimer. Gβ associates with Ste5 scaffold allowing activation of associated Ste11 (MAPKKK) by Ste20 (PAK), which is anchored at the plasma membrane through Cdc42 GTPase. Ste20 may also associate with and be stimulated by Gβ. Ste20 phosphorylates Ste11, allowing sequential phosphorylation of Ste7 (MAPKK) and Fus3/Kss1 (MAPK). The MAPKs (mainly Fus3) activate Ste12 (transcription factor) and Far1 (cyclin-dependent kinase inhibitor) to trigger growth arrest and shmoo formation.
(B) Morphology of *bni1Δ* cells before and after α factor treatment. WT (EY699) and *bni1Δ* (EYL427) cells were grown to A_{600} ≈0.6 at 30°C then treated with 5 μM α factor for 2 hours. The cells were fixed with 4% formaldehyde, briefly sonicated and then observed under the microscope. (C) *bni1Δ* cells do not undergo G1 arrest when exposed to α factor. Shown here is a halo assay of WT and *bni1Δ SST1* strains. Photo was taken after 36 hours. (D) Quantification of *bni1Δ* cell defects in α factor-induced G1 arrest, shmoo formation and mating. For G1 arrest and shmoo formation, cells were treated with α factor as in B. Over 300 cells were counted. For quantitative mating, WT and *bni1Δ* cells were mated to a MATα strain for 6 hours on YPD plates. Diploid formation was quantitated as the percentage of prototrophs formed between equal number of MATa and MATα cells. (E) α factor-activated transcription activation is suppressed in *bni1Δ* cells. EY699 and EYL427 strains harboring *FUS1-lacZ* (EBL95) were treated with α factor for 1.5 hours. β-Galactosidase assays were performed as described. Values (Miller units of β-galactosidase activity) are means ± s.d. of triplicate transformants. Error bars are too small to be seen for the *bni1Δ* values.

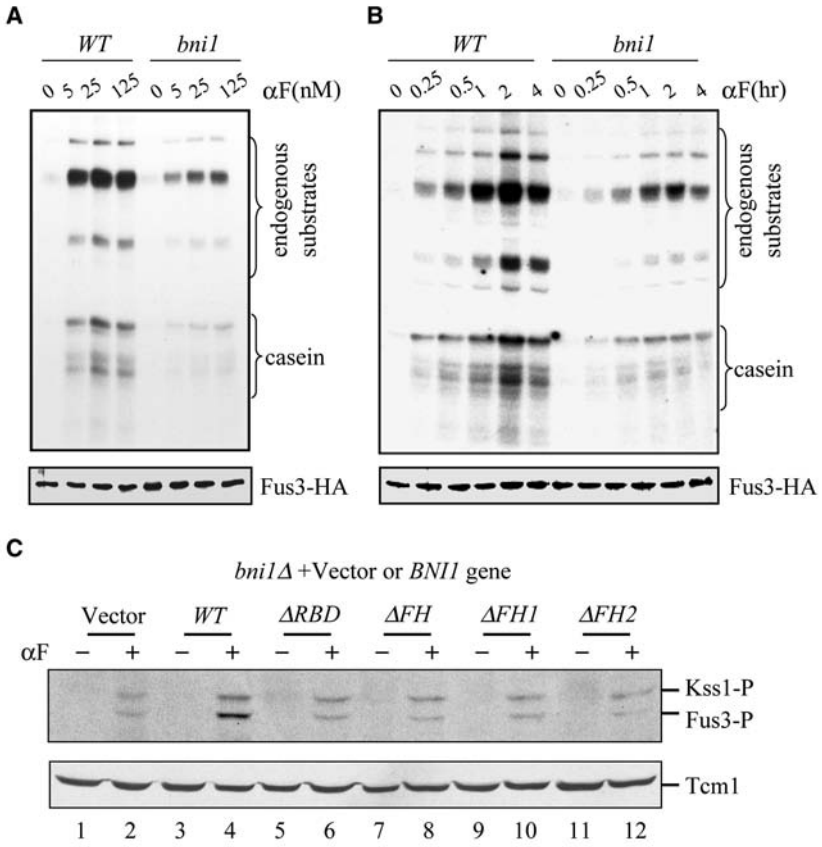

Fig. 2. *bni1Δ* cells are defective in α factor-induced Fus3 activation. (A) Dose dependence. WT (EY957) and *bni1Δ* (EYL917) cells harboring *FUS3-HA* (PYEE1102) were treated with different concentrations of α factor for 15 minutes and frozen at –80°C. (B) Time course. Cells were treated with 25 nM α factor for different lengths of time as indicated. Fus3 activation was monitored by in vitro kinase assay. Casein was used as a substrate. Upper bands are endogenous substrates that co-precipitate with Fus3-HA. (C) Effect of *bni1* deletion on Fus3 and Kss1 activation. *bni1Δ* strain (EYL917) was transformed with *CEN* plasmids harboring WT *BNI1* or *bni1* domain deletion mutants. The deletions are the RBD (*ΔRho*), both FH1 and FH2 domains (*ΔFH*), the FH1 domain (*ΔFH1*) and the FH2 domain (*ΔFH2*). Empty vector was also transformed as control. Cells were stimulated with 25 nM α factor for 15 minutes.

requirement for Bni1 in the pheromone response pathway (Evangelista et al., 1997) was done in a strain that had an *sst2Δ* mutation in the RGS protein that downregulates Gα (Gpa1) and has unnaturally high levels of free Gβγ (Siekhaus and Drubin, 2003). Our findings show that loss of Bni1 compromises multiple outputs of the mating MAPK cascade, suggesting it interferes with MAPK activation.

Dose–response curves and *fus3* mutant analysis suggest that increased Fus3 activation is required for transcriptional activation, G1 arrest and shmoo formation (Farley et al., 1999). Therefore, the partial defects in *FUS1-lacZ* expression and G1 arrest in a *bni1Δ* strain could be explained by a reduction in the level of Fus3 activation. Fus3 kinase activity was monitored in wild-type (WT) and *bni1Δ* strains that lack the *SST1/BAR1* protease, which degrades α factor, allowing the use of much lower amounts of α factor and bypassing the downregulatory effects of pheromone-induced expression of the Sst1/Bar1 protease. The *bni1Δ* mutation still caused a reduction in G1 arrest and *FUS1-lacZ* expression in the *sst1Δ* background, however a slightly smaller effect on *FUS1-lacZ* expression was detected (data not shown). A comparison of Fus3 activity in these cells confirmed that *bni1Δ* cells do not efficiently activate the mating MAPK cascade. Fus3 activity was lower in *bni1Δ* mutant cells than in WT cells at all α factor concentrations in a dose–response experiment, including saturating concentrations of α factor (25 nM and 125 nM; Fig. 2A). Furthermore, a time-course experiment showed that the reduced Fus3 activity was not the result of a delay in signal transduction. Fus3 was activated with similar kinetics in WT and *bni1Δ* cells, however, the overall level of activation was lower at all time points in the *bni1Δ* cells (Fig. 2B). Quantitation of multiple experiments by densitometry revealed an approximate fourfold reduction in Fus3 activity at various time points and α factor concentrations (Fig. S1 in supplementary material). Therefore, a *bni1Δ* mutant is intrinsically defective in α factor-induced MAPK activation.

We determined whether Bni1 was also required to activate Kss1, which does not need to be bound to Ste5 to be activated by mating pheromone (Andersson et al., 2004). The activation of endogenous Fus3 and Kss1 in whole cell extracts was monitored with an antiphospho p42p44 antibody that recognizes the active form of ERK1 and ERK2 in mammalian cells and cross-reacts with active Fus3 and Kss1 (Andersson et al., 2004). In the cells expressing wild-type *BNI1*, a stronger signal of active Fus3 than Kss1 was detected after α factor stimulation (Fig. 2C, lanes 3, 4). Strikingly, the level of active Kss1 was only slightly reduced in the *bni1Δ* strain, compared to a much larger reduction in the level of active Fus3 (Fig. 2C, lanes 1, 2). Thus, Bni1 is specifically required for high-level activation of Fus3.

Bni1 acts at, or upstream of, Ste5 in mating pathway signaling

Bni1 localizes at sites of polarized growth in dividing cells and in pheromone-stimulated cells (Evangelista et al., 1997; Ozaki-Kuroda et al., 2001), suggesting that it was likely to affect an aspect of Fus3 activation that takes place at the plasma membrane, near the receptor, G protein or Ste20 steps of the pathway (Fig. 1A). To determine whether Bni1 acts upstream or downstream of Ste20, we tested whether the *bni1Δ* mutation interferes with activation of Fus3 by a constitutively active form of MAPKKK Ste11, Ste11-4. Ste11-4 has a T596I mutation in subdomain VII (596TDFG599) of the catalytic domain that renders it able to activate Fus3 in the absence of the receptor, G protein and Ste20. The Ste11-4 protein confers a dominant phenotype and is still constitutively active in the presence of wild-type Ste11 (Stevenson et al., 1992). Expression of Ste11-4 at physiological levels partially suppressed the *bni1Δ* defect in Fus3 activation (Fig. 3A), such

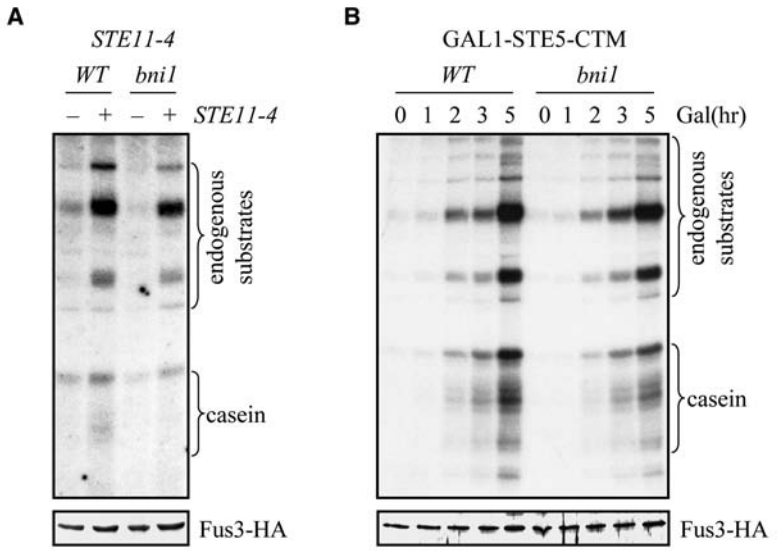

Fig. 3. *bni1* functions at or upstream of Ste5 in Fus3 activation. (A) Ste11-4-induced Fus3 activation of WT and *bni1Δ* cells. *STE11-4* was expressed in a *CEN* plasmid (EBL284) and empty vector was used as control. (B) Ste5-CTM-induced Fus3 activation. Ste5-CTM (EBL204) was expressed from the *GAL1* promoter. After shifting from raffinose to galactose medium, cells were collected at 0, 1, 2, 3 and 5 hours.

that the levels of Fus3 activation in the *bni1Δ* mutant approached that of the WT strain, suggesting that Bni1 functions near the Ste11 step. Ste5 was a probable target point because full activity of Ste11-4 is dependent upon recruitment of Ste5 (Andersson et al., 2004).

We therefore asked whether Bni1 regulates Fus3 at or upstream of the Ste5 recruitment step that is essential for Ste11 activation, by testing whether artificial recruitment of Ste5 to the plasma membrane bypasses the *bni1Δ* defect in Fus3 activation. This was done with Ste5-CTM, which localizes to the plasma membrane through a carboxyl-terminal transmembrane sequence and constitutively activates the mating MAPKs through a process that requires activation of Ste11 by Ste20, but bypasses the need for binding of Ste5 to the G protein (Pryciak and Huntress, 1998). This phenotype is dominant and detected in the presence of wild-type Ste5. WT and *bni1Δ* cells were shifted to galactose medium to induce the expression of Ste5-CTM and Fus3 kinase activity was monitored. Ste5-CTM-activated Fus3 nearly identically in *bni1Δ* and WT cells (Fig. 3B). Therefore, Bni1 regulates Fus3 activation at or upstream of Ste5 recruitment.

Bni1 is required for cortical recruitment of Ste5 during pheromone stimulation

We determined whether *bni1Δ* mutants were defective in localizing Ste5 to cortical sites on the plasma membrane during α factor stimulation in a time-course experiment. Cortical recruitment of Ste5 was analyzed in live cells with a functional Ste5-GFP fusion expressed at the same level as wild-type Ste5 using the *CUP1* promoter (Mahanty et al., 1999). The recruitment of Ste5-GFP was severely defective in *bni1Δ* cells at all time points after α factor addition, including the 15 minute time point that is well before shmoo formation (Fig. 3A,C). In WT cells after 15 minutes of α factor treatment, Ste5-GFP could be detected at the plasma membrane (rim staining) in ~12% of the population (Fig. 3C). These cells had not undergone shmoo formation and were still round. As the length of α factor exposure increased, the number of cells that exhibited Ste5 rim staining also increased, with more intense staining at emergent shmoo tips. After 2 hours of exposure to α factor, ~90% of the cells formed shmoos, and strong Ste5 rim staining was detected in 67% of cells. In contrast, Ste5 recruitment was greatly reduced in *bni1Δ* cells at all time points. Similar results were found by indirect immunofluorescence of a functional Ste5-Myc9 fusion in fixed cells (Fig. 3B,D). Ste5 was recruited to wild-type levels in a *bnr1Δ* strain lacking Bnr1, the homolog of Bni1 (data not shown) and in *she* mutant strains (including *she5*, which is allelic to *bni1*) defective in polarized localization of specific mRNAs (Fig. S2 in supplementary material). Thus, Bni1 plays a critical role in Ste5 recruitment that is not performed by Bnr1 and is distinct from proteins involved in polarized mRNA localization.

Bni1 is still required for recruitment of Ste5 after the Fus3 signaling defect is suppressed

Ste5 relocalizes from the nucleus to the plasma membrane in response to α factor stimulation of the associated MAPK cascade (Mahanty et al., 1999). Therefore, it was possible that the defect in Ste5 localization in the *bni1Δ* mutant was a secondary consequence of a defect in MAPK activation. To test this possibility, we restored wild-type levels of Fus3 activation in a *bni1Δ* mutant by expressing Ste5-CTM from the *GAL1* promoter that is induced in the presence of galactose, and examined whether Ste5-Myc9 could now be recruited to the plasma membrane. In WT cells, the expression of Ste5-CTM was sufficient to induce translocation of Ste5-Myc9 from the nucleus to the emerging shmoo tip (Fig. 4F,G, percentage nuclear accumulation and percentage rim staining), demonstrating that activation of the MAPK cascade is sufficient to induce Ste5 relocalization. (Note that it is easier to see the nuclear pool of Ste5 when cells are grown in galactose containing medium than in glucose containing medium; P. Maslo, R. McCully, E.A.E., unpublished data.) Ste5-CTM did not induce recruitment of Ste5-Myc9 in *bni1Δ* cells; Ste5-Mcy9 remained predominantly nuclear despite nearly wild-type levels of Fus3 activation (Fig. 4E-G). Thus, Bni1 regulates recruitment of Ste5 by a mechanism that is independent of MAPK activation. Furthermore, the retention of Ste5 in nuclei of the *bni1Δ* cells indicates that Bni1 also promotes redistribution of Ste5 from the nucleus to the cytoplasm and cell cortex.

Bni1 is required for cortical recruitment of Fus3 and Cdc24, but not Ste20

In parallel experiments, we looked at the localization of Fus3, whose recruitment is dependent on Ste5. In WT cells, Fus3-GFP was nuclear and cytoplasmic and accumulated at shmoo

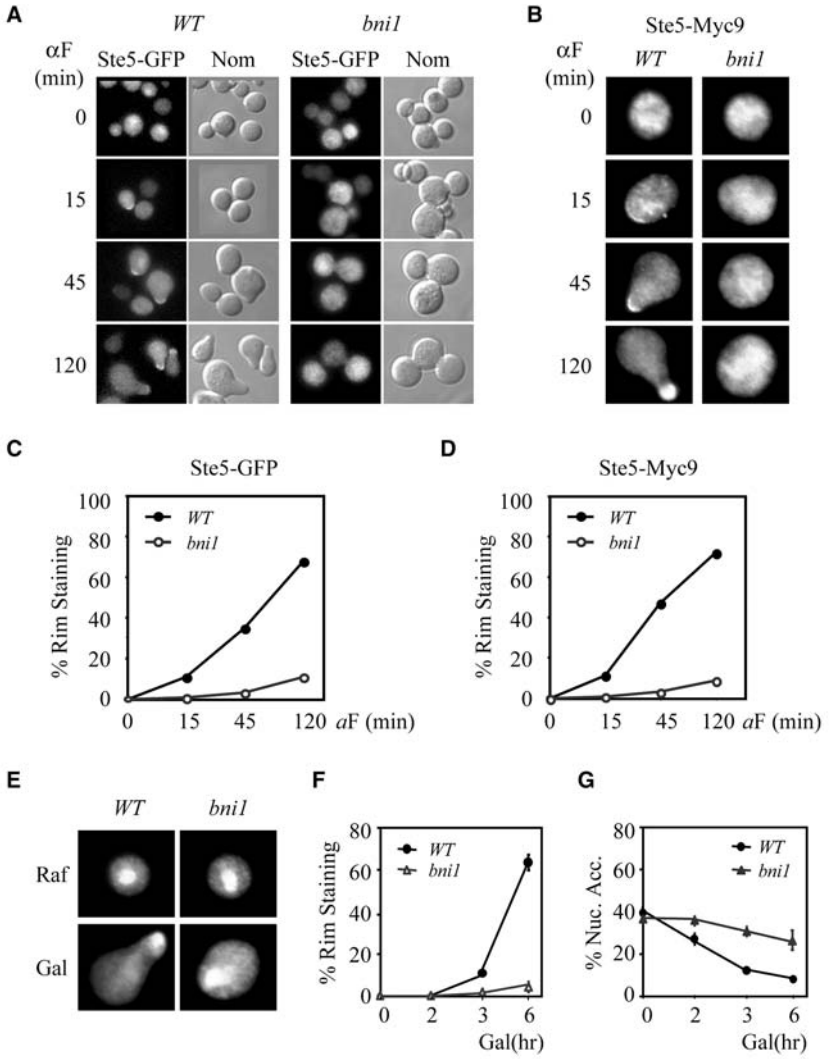

Fig. 4. *bni1* is required for Ste5 recruitment to the cell cortex. (A) Time course of Ste5-GFP localization in WT and *bni1Δ* cells. Cells (EY699 and EYL427) expressing Ste5-GFP (EBL367) from the *CUP1* promoter were induced with 500 μM $CuSO_4$ for 2 hours, then treated with 50 nM α factor. An aliquot of cells was fixed at 15, 45 and 120 minutes in 4% formaldehyde. Cells were briefly sonicated and then observed under the microscope. Nomarski images (Nom) show cell morphology. (B) Ste5-Myc9 localization in WT (filled circles) and *bni1Δ* (open circles) cells. EY957 and EYL917 expressing Ste5-Myc9 (EBL453) were treated with 50 nM α factor and fixed in 4% formaldehyde and indirect immunofluorescence was conducted to detect Myc. (C) Quantitation of Ste5-GFP localization in WT and *bni1Δ* cells. Cells were treated as in A. Values represent averages of two independent experiments. Up to 200 cells were counted for each condition. (D) Quantitation of Ste5-Myc9 localization in WT and *bni1Δ* cells. Values represent averages of two independent experiments. Up to 300 cells were counted for each condition. (E) Ste5-CTM cannot induce Ste5-Myc9 translocation in *bni1Δ* cells. WT (EY957) and *bni1Δ* (EYL917) cells were transformed with Ste5-CTM (EBL204) and Ste5-Myc9 (EBL365). Cells were pregrown in 2% raffinose overnight, shifted to 2% galactose to induce Ste5-CTM expression. Aliquots of cells were fixed at 2, 3 and 6 hours and Myc was detected by indirect immunofluorescence. (F) Quantitation of Ste5-Myc9 cortical localization in Ste5-CTM-induced cells. Ste5-Myc9 rim staining in WT (filled circles) and *bni1Δ* (open triangles) were counted in over 300 cells. (G) Quantitation of Ste5-Myc9 nuclear localization in Ste5-CTM-induced cells. Ste5-Myc9 nuclear accumulation in WT (filled circles) and *bni1Δ* (filled triangles) were counted in over 300 cells.

tips only after long-term treatment with α factor. In contrast, no cortical recruitment of Fus3-GFP was detected at all in the *bni1Δ* cells (Fig. 5A middle panels, B). Consistent with these findings, we found that the cortical pool of Ste5 always co-localizes with Bni1, with ectopic expression of Bni1 modestly enhancing basal and pheromone-induced cortical recruitment of Ste5 and both basal and pheromone-induced activation of Fus3 (data not shown). Thus, Bni1 is critical for recruitment of Fus3 in addition to Ste5.

We assessed whether Ste20 was still recruited in *bni1Δ* cells to determine whether loss of Bni1 globally interferes with cortical localization during the pheromone response. Ste20 accumulates at the cell cortex by binding to Cdc42 through a CRIB motif (Cdc42-Rac interactive binding motif) (Lamson et al., 2002). The *bni1Δ* mutation did not block cortical recruitment of Ste20-GFP, which localized to the cortex in a polarized manner in *bni1Δ* cells that had been treated with α factor to the same degree as WT cells, even though the cells were blocked in shmoo formation and round (Fig. 5A lower panels, 5B). Therefore, Cdc42-mediated asymmetry still exists in *bni1Δ* cells that have lost polarization of the actin cytoskeleton and cannot undergo polarized growth.

The guanine exchange factor Cdc24 also binds Cdc42 in addition to Ste5 and is required for polarized recruitment of Ste5. In contrast to Ste20, cortical recruitment of Cdc24 was greatly inhibited in the *bni1Δ* mutant during pheromone stimulation, although it was still recruited during mitotic growth (Fig. 5C,D). Similar results were found for Bem1 (data not shown), which has previously been shown to be dependent on the actin cytoskeleton for cortical recruitment during pheromone stimulation (Ayscough and Drubin, 1998) and forms complexes with both Ste5 and Cdc24 (reviewed by Wang et al., 2005). Thus, Bni1 is required for cortical recruitment of Cdc24 during pheromone stimulation, consistent with the possibility that Cdc24 and Ste5 are recruited as a complex (Wang et al., 2005).

The Rho1-binding domain and FH domains in Bni1 regulate MAPK activation

Bni1 is a large protein with many domains that bind directly or indirectly to a variety of proteins including Rho GTPases (i.e. Rho1, Rho3 and Rho4), Cdc42, Spa2, profilin, actin, EF1α and Bud6 (Fig. 6A) (Evangelista et al., 1997; Evangelista et al., 2002; Sagot et al., 2002). During mitotic cell division, Cdc42 regulates cortical recruitment of Bni1 potentially with

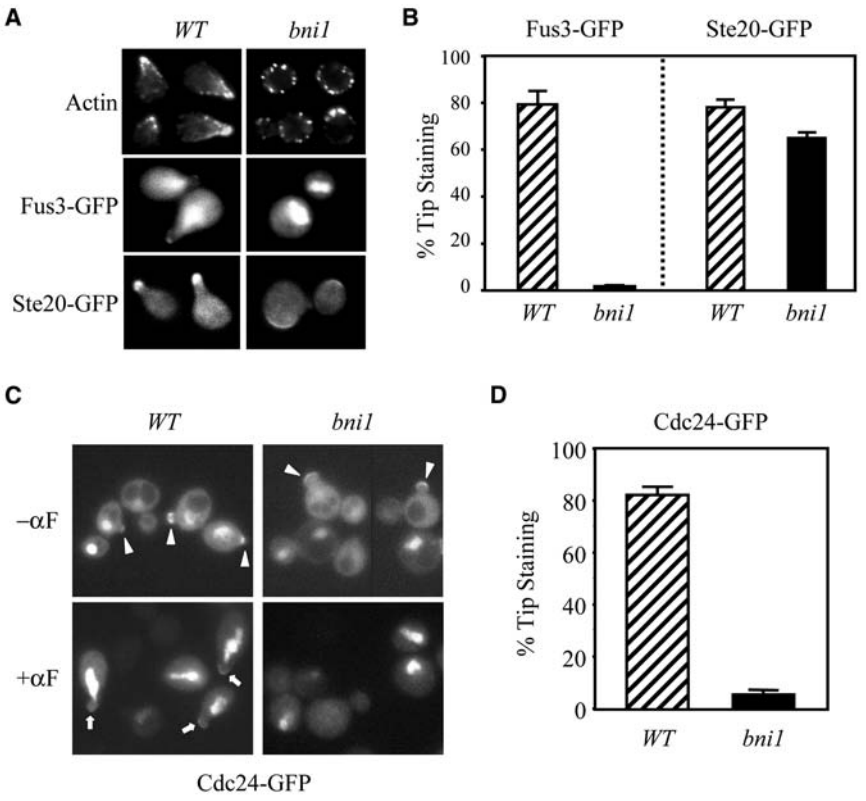

Fig. 5. *bni1* is required for Fus3, but not Ste20 recruitment. (A) Recruitment of Fus3 and Ste20 in *bni1Δ* strain. Upper panels: actin staining. WT (EY957) and *bni1Δ* (EYL917) cells were treated with 50 nM α factor for 2 hours, fixed, and then stained with Rhodamine-phalloidin. Middle panels: Fus3-GFP. Lower panels: Ste20-GFP. Strains expressing genomic Fus3-GFP (EYL1096 and QMY27) or strains (EY957 and EYL917) transformed with GFP-Ste20 (EBL511) were treated with 50 nM α factor for 2 hours, fixed with 4% formaldehyde, sonicated and then mounted for microscopy. (B) Quantitation of Fus3-GFP and Ste20-GFP localization in WT and *bni1Δ* cells. Values represent mean ± s.d. of two transformants. (C,D) Bni1 is recruited for Cdc24 recruitment during mating. WT (EY957) and *bni1Δ* (EYL917) strains were transformed with *CDC24*-GFP (EBL664). Cells were pregrown overnight in medium containing 0.19 mM methionine, then treated with 50 nM α factor for 2 hours. Note that Cdc24 localizes at bud tips (arrowheads) and shmoo tips (arrows). Over 200 cells were counted. Values in D represent mean ± s.d. of two transformants.

multiple Rho proteins (Jacquenoud and Peter, 2001; Dong et al., 2003). The control by Cdc42 is indirect compared to that of Rho1, which is sufficient to stimulate plasma membrane recruitment of Bni1 (Jacquenoud and Peter, 2000). Bni1 promotes actin cable formation through the FH1 and FH2 domains and is thought to exist in an autoinhibited form via interactions between the Rho-binding domain (RBD) and a carboxyl-terminal domain (DAD), by analogy to Diaphanous-related formin (Zigmond, 2004). The binding of Rho GTPase is thought to relieve the autoinhibitory interaction and permit the FH2 domain to nucleate actin polymerization (Evangelista et al., 2002; Sagot et al., 2002).

We deleted these key functional domains of Bni1 and assessed their role in Fus3 activation (Fig. 2C) and mating outputs (data not shown). As summarized in Table 1, deletion of the DAD that binds the RBD and Bud6 did not block mating responses, whereas removing the RBD did. Loss of the RBD also reduced Fus3 activation to the same degree as a *bni1* null strain (Fig. 2C) and blocked shmoo formation (percentage shmoos after 2 hours in 50 nM α factor was 80% for WT, 0.01% for *bni1Δ*, 0.03% for *bni1ΔRBD*; *n*=300 cells; see also Fig. 6B). Furthermore, deletions that removed the FH1 and FH2 domains also inhibited Fus3 activation (Fig. 2C) and mating outputs. These findings suggest that Bni1 regulation of Ste5 recruitment requires a Rho GTPase and the formation of actin cables.

To test this hypothesis, we determined whether the RBD was required for cortical localization of Bni1. The RBD (amino acid residues 90-343) has been defined as a region that binds Rho1-GTP directly in vitro and in two-hybrid assays (Kohno et al., 1996). This region overlaps the region of Bni1 with homology to the Diaphanous GTPase binding domain (amino acids 93-286) (Marchler-Bauer et al., 2003). Bni1 lacking the RBD (*bni1ΔRBD*-GFP) did not localize to bud tip and bud neck during vegetative growth and was not recruited to the cell cortex during response to mating pheromone, even in cells that expressed wild-type Bni1 (Fig. 6B). Consistent with the absence of cortical recruitment, *bni1ΔRBD*-GFP failed to support shmoo formation in *bniΔ* cells (Fig. 6B), or mediate cortical recruitment of Ste5 (data not shown).

The requirement for the RBD for Bni1 localization and pheromone responses suggested that Bni1 is activated during mating by a Rho GTPase. Five Rho GTPases (Rho1-Rho5) are implicated in the regulation of Bni1, with varying roles during the cell cycle and under different environmental conditions (Dong et al., 2003). Although early work with a temperature sensitive *rho1-2* mutant suggested that Rho1 is not involved in localization of Bni1 (Ozaki-Kuroda et al., 2001), other work has shown that Rho1 regulates the actin cytoskeleton during G1 phase and shmoo formation (Kohno et al., 1996; Drgonova et al., 1999), and binds to multiple effector proteins including Bni1, glucan synthase and protein kinase C (Evangelista et al., 1997; Saka et al., 2001). We compared Bni1 and Ste5 localization in *rho1-2* (E45V in Switch I) (Saka et al., 2001) and *rho1-104* (D72N; C164Y) (Yamochi et al., 1994) temperature sensitive mutants that have different actin cytoskeleton phenotypes and abilities to polarize myosin. Bni1-GFP was not recruited in a polarized manner to the cortex of dividing and pheromone-induced *rho1-2* and *rho1-104* cells at nonpermissive temperature (Fig. 6C). To determine whether Rho1 was also required for Ste5 localization we used TAgNLS^{K128T}-Ste5-Myc9, which is more efficiently reimported to the nucleus and recruited to the plasma membrane than Ste5-Myc9, allowing its detection in a greater

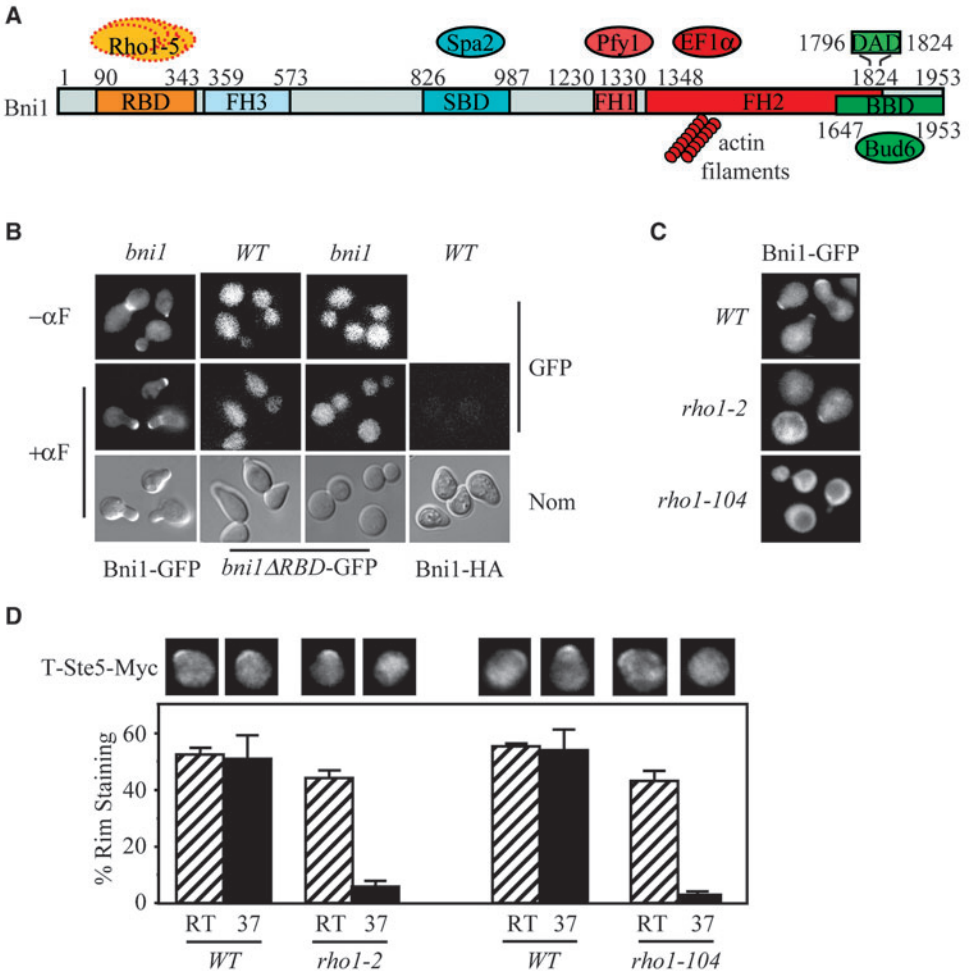

Fig. 6. Rho1 is involved in Bni1-mediated Ste5 recruitment. (A) Schematic structure of Bni1. RBD, Rho-binding domain; SBD, Spa2-binding domain; BBD, Bud6-binding domain. (B) Rho-binding domain is required for Bni1 polarization. WT cells were transformed with *bni1ΔRBD*-GFP (QMB79) or *BNI1-HA* (EBL332); *bni1Δ* cells were transformed with *BNI1*-GFP (EBL334) or *bni1ΔRBD*-GFP (QMB79). Cells were treated with 50 nM α factor for 2 hours, then direct fluorescence of GFP was observed. Nomarski images (Nom) show cell morphology. (C) Bni1 polarization is defective in *rho1-TS* mutants. WT (QMY550), *rho1-2* (QMY553) and *rho1-104* (QMY551) cells expressing Bni1-GFP were grown at room temperature. Cells were shifted to 37°C for 1 hour, then induced with 5 μM α factor at 37°C or 2 hours. (D) Ste5 recruitment is defective in *rho1-TS* mutants. WT, *rho1-2* and *rho1-104* cells expressing TAgNLS^{K128T}Ste5-Myc9 (EBL444) were treated as in C, except the α factor stimulation time was 30 minutes. Cells were fixed and Myc was detected by indirect immunofluorescence microscopy. Values represent mean ± s.d. of two transformants.

number of cells after brief treatment with α factor (Mahanty et al., 1999). Strikingly, the *rho1-2* and *rho1-104* mutations both decreased Ste5 recruitment at nonpermissive temperature (Fig. 6D). By contrast, Bni1 and Ste5 were still recruited to the site of polarized growth in *rho2*, *rho3*, *rho4* and *rho5* null mutants that had been treated with α factor, and these cells were able to form shmoos (Fig. S3 in supplementary material). Therefore, Rho1 specifically recruits Bni1 to cortical sites during mating and positively regulates recruitment of Ste5 through control of Bni1.

Bni1-induced actin cables are required for Ste5 recruitment

To more stringently test for a primary role of Bni1-induced cables in Ste5 recruitment, we used a *bni1^{TS}* temperature-sensitive mutation within conserved residues of the FH2 domain (R1528A and R1530A) that blocks actin cable formation (Sagot et al., 2002). Previous work has demonstrated that inactivation of *bni1^{TS}* after a brief 10-minute shift to 34°C selectively disrupts actin cables while polarized actin patches are maintained, although the effect is not complete. Because of partial functional overlap between Bni1 and Bnr1, the *bni1^{TS}* mutation was assessed in a *bnr1Δ* mutant as described (Evangelista et al., 2002; Sagot et al., 2002). At the nonrestrictive temperature, TAgNLS^{K128T}-Ste5-Myc9 was recruited to the plasma membrane in ~30% of WT and *bni1^{TS} bnr1Δ* mutant cells after α factor stimulation (Fig. 7A). Shifting the temperature to 34°C greatly inhibited the recruitment of TAgNLS^{K128T}-Ste5-Myc9 in the *bni1TSbnr1Δ* mutant, but did not reduce it in the WT control strain (Fig. 7A), consistent with a primary role for actin cables in Ste5 recruitment.

To further confirm that actin cables regulate Ste5 recruitment, we checked the effect of disrupting the *TPM1* and *TPM2* genes encoding tropomyosins, which bind to and stabilize actin cables and are not a component of actin patches (Pruyne et al., 1998). To assess the immediate importance of

Table 1. Phenotypes of *bni1* mutants

Genotype	Pheromone response
WT	++++
bni1Δ	+
bni1ΔRBD	+
bni1ΔFH1/FH2	+
bni1ΔFH1	++
bni1ΔFH2	++
bni1ΔCT	++++

WT, wild type. *bni1Δ* cells were transformed with empty vector, or vector expressing different forms of the *BNI1* gene. Sensitivity to α factor was monitored by Fus3 kinase assay and halo assay.

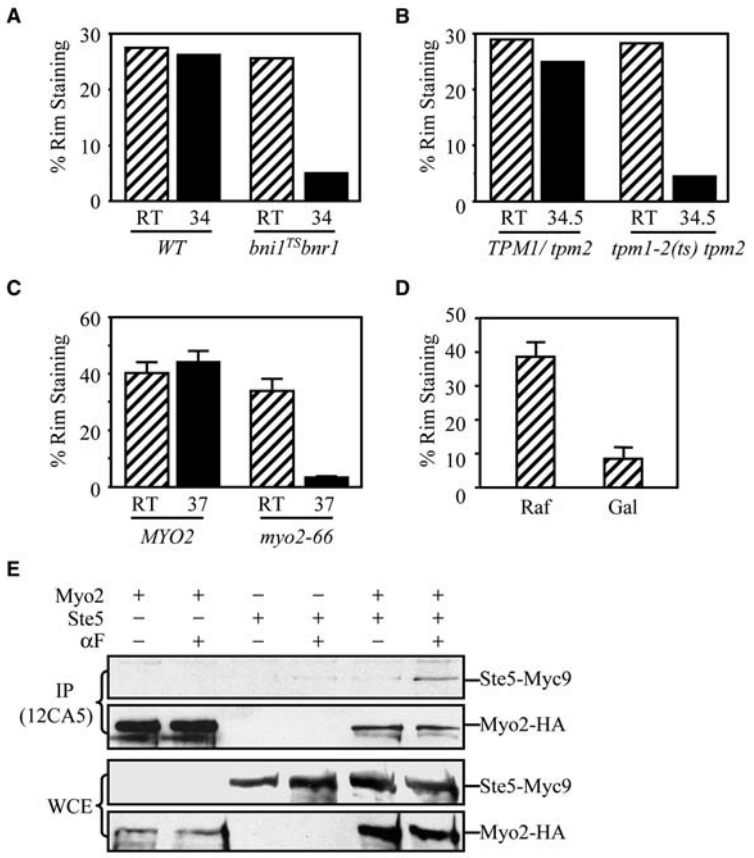

Fig. 7. *bni1* regulates Ste5 relocalization by controlling actin cable formation. (A) The *bni1*^{TS} mutant cannot recruit Ste5. WT (EYL1765) and *bni1*^{TS} *bnr1Δ* (EYL1748) cells expressing TAgNLS^{K128T}Ste5-Myc9 were grown at room temperature. Cells were centrifuged, resuspended in pre-warmed medium (34°C) containing 5 μM α factor, and then incubated at 34°C for 10 minutes. (B) The *tpm1*^{TS} mutant cannot recruit Ste5. TAgNLS^{K128T}Ste5-Myc9 was expressed in *tmp2Δ* (EYL1736) and *tpm1*^{TS}*/tmp2Δ* (EYL1735) mutant cells. Cells were then treated as in A, except at a nonpermissive temperature of 34.5°C. Values in A and B represent mean of two independent experiments. (C) Ste5 recruitment is inhibited in *myo2-66* cells at nonpermissive temperature. *MYO2* (QMY458) or *myo2-66* (QMY459) cells expressing TAgNLS^{K128T}Ste5-Myc9 (EBL444) were grown at room temperature, then incubated at 37°C for 2 hours, treated with 5 μM α factor for 30 minutes, then fixed for indirect immunofluorescence.
(D) Overexpression of Myo2 tail domain suppresses Ste5 recruitment. Cells harboring *MYO2DN* (QMB75) and TAgNLS^{K128T}Ste5-Myc9 (EBL444) were pre-grown in medium containing 2% raffinose overnight. The cells were shifted to medium containing 2% galactose for 1 hour, treated with 5 μM α factor for 15 minutes, then fixed and Myc was detected by indirect immunofluorescence microscopy. (E) Ste5 co-immunoprecipitates with Myo2 in α factor-treated cells. EY1775 (*ste5Δ*) expressing Ste5-Myc9 (from EBL358) and/or Myo2-HA (from QMB80), with or without control vectors, were grown to early logarithmic phase. Where indicated (+), cells were treated with 50 nM α factor for 45 minutes prior to collecting cells for extract preparation. 12CA5 and 9E10 monoclonal antibodies were used to detect Myo2-HA and Ste5-Myc9, respectively. Note the nonspecific binding of Ste5 to Sepharose beads.

tropomyosin in Ste5 recruitment, we used the same rapid temperature shift conditions used for the *bni1*^{TS} mutant. Although TAgNLS^{K128T}-Ste5-Myc9 was recruited to the cortex in *tpm1*^{TS} *tpm2Δ* cells at nonrestrictive temperature, shifting to nonpermissive temperature blocked its recruitment within a few minutes (Fig. 7B). Thus, actin cables generated by Bni1 and stabilized by tropomyosin are required for recruitment of Ste5 to polarized sites at the plasma membrane.

Myo2 is required for recruitment of Ste5

All of the known transport events along actin cables in *S. cerevisiae* require either of the type V myosin motor proteins, Myo2 and Myo4. Myo2 has been implicated in the transport of proteins (i.e. Kar9, Smy1) and organelles (i.e. secretory vesicles and vacuoles) along cytoplasmic actin cables, whereas Myo4 is involved in transport of mRNAs to sites of polarized growth (Bretscher, 2003; Vale, 2003). We used two approaches to test whether Myo2 is involved in Ste5 recruitment, a *myo2-66* temperature-sensitive point mutation that maps to the actin-binding region of the motor domain of Myo2 (Lillie and Brown, 1994) and a dominant negative tail fragment of Myo2, *MYO2DN* that displaces Myo2 from actin cables (Reck-Peterson et al., 1999). Shifting the *myo2-66* strain to 37°C for 2 hours blocked recruitment of Ste5 (Fig. 7C). Since the *myo2-66* mutation also induces actin depolarization in addition to inactivating Myo2, we examined the effect of *MYO2DN* under conditions of short-term overexpression from the *GAL1* promoter, which does not disrupt the actin cytoskeleton (Reck-Peterson et al., 1999; Karpova et al., 2000). Shifting cells from noninducing raffinose medium to inducing galactose medium for 1 hour resulted in a fourfold inhibition of recruitment of TAgNLS^{K128T}-Ste5-Myc9 in the presence of α factor (Fig. 7D). Thus, Ste5 recruitment was blocked to nearly as great an extent by *MYO2DN* as it was by *myo2-66*. A comparative analysis of Ste5 recruitment in strains harboring mutations in the remaining myosin genes, *MYO1, MYO3, MYO4* and *MYO5* [of which *MYO3* and *MYO5* are functional homologs (Bretscher, 2003; Vale, 2003)] was also done. Deletion of *MYO4,* in either a WT or *myo2-66* background did not interfere with Ste5 recruitment (Fig. S4A in supplementary material). Furthermore, null mutations in *MYO1*, *MYO3, MYO5* and double null mutations in *MYO3 MYO5* had no significant effect on Ste5 recruitment (Fig. S4B,C in supplementary material). Thus, Myo2 is specifically required for cortical recruitment of Ste5.

The actin cables and Myo2 could regulate Ste5 recruitment indirectly by creating a polarized site of factors that capture and stabilize Ste5. Alternatively, it is possible that Myo2 played a more direct role through translocation of Ste5 along actin cables. To test the possibility that Myo2 might regulate translocation of Ste5 we determined whether Ste5 and Myo2 form complexes in vivo in a co-immunoprecipitation assay. Ste5-Myc9 and Myo2-HA were co-expressed in a *ste5Δ* strain at physiological levels using low copy centromeric plasmids and *STE5* and *MYO2* promoters to drive the expression of *STE5-MYC9* and *MYO2-HA* genes, respectively. Strikingly, Myo2-HA associated with Ste5-Myc9 in cells that had been

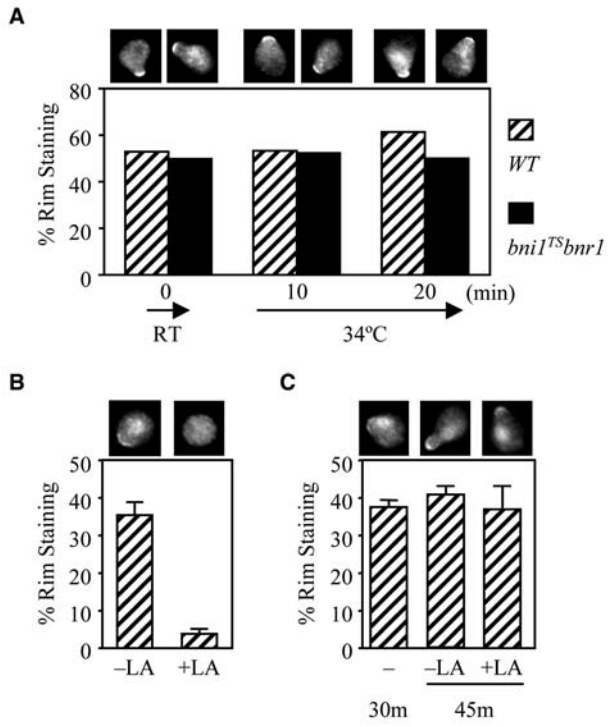

Fig. 8. Actin is not required to keep Ste5 at the plasma membrane. (A) Dynamics of Ste5 localization in *bni1*^{TS} mutants. WT (EYL1765) and *bni1*^{TS}*bnr1Δ* cells (EYL1748) expressing TAg^{NLSK128T}Ste5-Myc9 were treated with 5 μM α factor at room temperature for 30 minutes, and then shifted to 34°C for 10 minutes and 20 minutes. Values are means of two independent transformants. Two separate experiments gave comparable results. (B) Actin filaments are required to recruit Ste5. WT (EY957) cells harboring TAg^{NLSK128T}Ste5-Myc9 were treated with 100 μM latrunculin A (Lat A) for 15 minutes, then treated with 50 nM α factor for 15 minutes. (C) Ste5 dynamics in Lat A-treated cell. Cells as used in B were treated with 50 nM α factor for 30 minutes, then Lat A was added to the medium at a final concentration of 100 μM. The cells were further incubated for 15 minutes before fixed for immunofluorescence. Values are mean ± s.d. from three independent experiments.

treated with α factor but not in vegetatively growing cells (Fig. 7E), consistent with the dependence of polarized recruitment of Ste5 on α factor stimulation. The ability to co-immunoprecipitate Ste5 and Myo2 was reproducible and dependent on expressing Myo2 at native levels, with no interaction detected when Myo2 was overexpressed (data not shown). Collectively, these findings open the possibility that Ste5 translocates along actin cables through the action of Myo2.

Ste5 does not need the Bni1 FH2 domain or actin to stay at the plasma membrane

We determined whether Bni1 or actin cables were required to maintain Ste5 at the cell cortex once it has been recruited to Gβ Ste4. To test this possibility, the effect of the *bni1*^{TS} mutation and latrunculin A treatment on a pool of Ste5 that had been recruited to the cell cortex was assessed. *bni1*^{TS} *bnr1Δ* mutant cells expressing TAgNLS^{K128T}-Ste5-Myc9 were treated with α factor for 30 minutes at room temperature, then shifted to 34°C for 10 minutes and 20 minutes. The treatment with α factor induced Ste5 recruitment in 50% of the cells (Fig. 8A). The subsequent shift to 34°C blocked a further increase in recruitment of Ste5 to the polarization sites, but did not decrease the pool of Ste5 that had accumulated prior to the temperature shift (Fig. 8A). Therefore, once Ste5 is recruited to the plasma membrane, it no longer needs the FH2 domain of Bni1. The addition of latrunculin A prior to α factor induction completely blocks the formation of actin patches and cables and α factor-induced actin polarization as well as recruitment of Ste5 to the plasma membrane (Wang et al., 2005) (Fig. 8B). In sharp contrast, addition of latrunculin A to α factor-induced cells did not abolish the previously established Ste5-Myc9 recruitment (Fig. 8C), although it did disrupt the actin cytoskeleton, further demonstrating that the actin cytoskeleton is not required to maintain Ste5 at the plasma membrane. Therefore, Bni1-induced actin cables are not required to maintain Ste5 at the plasma membrane.

Discussion

While it is known that regulators of the actin cytoskeleton are required for signal transduction during MAPK signaling, specific functions of actin in signaling have not been delineated. Here we present the first evidence of a specific role for a formin and Rho protein in assembly of a scaffold-kinase signal transduction cascade at the plasma membrane in response to an external stimulus. This conclusion is based on the selective requirement for Bni1 in high-level activation of MAPK Fus3, but not MAPK Kss1 (Fig. 2), together with the critical role for Bni1 in cortical recruitment of Ste5 and Fus3 (Figs 4 and 5). Previous work suggests that Fus3 must be activated while bound to Ste5 (Andersson et al., 2004) but Kss1 can be activated from the scaffold by upstream kinases (Andersson et al., 2004; Maleri et al., 2004). In addition, plasma-membrane-bound Ste5-CTM does not recruit Kss1 to the plasma membrane although it does recruit Fus3 (van Drogen et al., 2001). Thus, Bni1 and cortical localization of Ste5 only play a significant role in the MAPK that co-localizes with Ste5. Although Bni1 and actin cables are required for polarized recruitment of Ste5 (Figs 4 and 7), they are not required for maintenance of Ste5 at the plasma membrane (Fig. 8). This finding is consistent with the expectation that once recruited, Ste5 is able to bind to free Gβ (Ste4) at the plasma membrane.

Our findings also reveal that Rho1 plays a specific role in mediating the recruitment of Bni1 and Ste5, acting through the Rho Binding Domain of Bni1 (Fig. 6). This conclusion is consistent with the ability of Rho1-GTP to bind to a Bni1 fragment that overlaps the Rho binding domain (Kohno et al., 1996) and the lack of evidence of functional overlap from the other Rho proteins (Rho2, Rho3, Rho4, Rho5, Fig. S3 in supplementary material), which may regulate Bni1 during the budding cycle (Dong et al., 2003). During the mitotic cycle, Rho1 also regulates the actin cytoskeleton indirectly through the protein kinase C pathway (Dong et al., 2003), raising the possibility of an indirect link between Rho1 and Bni1 during mating pheromone stimulation. However, the protein kinase C pathway is activated by α factor much later than the mating

MAPK cascade, as a result of polarized growth (Buehrer and Errede, 1997; Zarzov et al., 1996), arguing against this possibility. Interestingly, it was recently reported that Rho1 associates with Ste4 in co-immunoprecipitates (Bar et al., 2003), raising the possibility that Gβγ recruits Rho1 to the site of polarized growth during mating. Taken together with our findings, we speculate that Gβγ directs polarized growth through dual recruitment of a Rho1-GTP-Bni1 complex, which facilitates polarized growth directly through actin cable formation, as well as through recruitment of Ste5.

A major question that still remains is how Ste5 is recruited in a polarized manner. One possibility is that Ste5 is exported from the nucleus either alone or in a complex with Cdc24 and simply diffuses to the cortex where it is captured by cell polarity factors such as Cdc42 and Bem1 whose localization is also dependent on Bni1. The position of these factors could be determined by the asymmetry that is established from the receptor and activated G protein and polarized actin that assembles in response to the external pheromone stimulus. Such asymmetry could be built through an interaction between Ste4 and Rho1, which binds to Bni1. Potential direct or indirect interactions between Bni1 and Cdc42 (Evangelista et al., 1997; Jaquenoud and Peter, 2000) might serve to link the Bni1 complex to Ste5-Cdc24. This possibility is consistent with our ability to co-immunoprecipitate Bni1 with Bem1 (M.Q. and E.A.E., data not shown).

Another interesting possibility that is consistent with our findings is that a pool of Ste5, either alone or with Cdc24, translocates along actin cables once it is exported from the nucleus. This possibility is consistent with the requirement for the cargo domain of Myo2 in Ste5 recruitment and the ability to co-immunoprecipitate Ste5 with Myo2. While it is possible that the interaction between Myo2 and Ste5 is indirect, it is noteworthy that we can detect it, in light of the fact that we are unable to co-immunoprecipitate Bni1 with Ste5. Additional support for the physiological relevance of this interaction comes from the observation that the interaction is not detected when Myo2 is overexpressed (data not shown) and that it is dependent upon pheromone signaling. Prior work has implicated Myo2 in the translocation of secretory vesicles, vacuoles and several cytoskeleton-associated proteins (i.e. Kar9 and Smy1) (Vale, 2003) but not the translocation of a cytoplasmic protein. Additionally, the possibility that Ste5 translocates along actin cables with Myo2 is still consistent with a model in which Ste5 is captured at the cell cortex by cell polarity proteins. While further work is needed to know whether Ste5 is translocating along actin cables, this interpretation is attractive in that it provides a physical link between nuclear export and events at a specific site at the cell cortex. Interestingly, concentration of JIP scaffolds at nerve terminals requires kinesin, suggesting they translocate along microtubules via a direct interaction with kinesin (Verhey et al., 2001), although the reason for this phenomenon has not been established.

Finally, previous work has shown that Fus3 is required for cortical recruitment of Bni1 (Matheos et al., 2004). Our unpublished findings are consistent with Fus3 being required for cortical recruitment of Ste5 in G1 phase of the cell cycle (M.Q. and E.A.E., unpublished). This finding raises the possibility that the formation of a stable signaling complex is a downstream event that occurs after initial pathway activation by mechanisms that are dependent on the Bni1-induced actin cytoskeleton. Further work is needed to clarify the relative position of MAPK activation with formation of a stable Ste5 scaffold signaling complex and whether polarized recruitment of Ste5 plays a specific role in events that take place at the shmoo tip, including polarized growth.

We are extremely grateful to: C. Moon, B. N. Lee and S. Mahanty, who made the initial observations that *bni1Δ* mutant is defective in G1 arrest, Fus3 activation and Ste5 recruitment, respectively. We thank C. Boone, D. Pellman, A. Bretscher, R. Li, L. Weisman and A. Levchenko for yeast strains and plasmids used in this study. We thank D. Pellman and D. Lew for comments on the manuscript. This research was supported by National Institutes of Health grant GM46962, a Taplin Funds for Discovery Award, and American Heart Grant 0150175N to E.A.E.

References

Arkowitz, R. A. (1999). Responding to attraction: chemotaxis and chemotropism in Dictyostelium and yeast. *Trends Cell Biol.* **9**, 20-27.

Andersson, J., Simpson, D. M., Qi, M., Wang, Y. and Elion, E. A. (2004). Differential input by Ste5 scaffold and Msg5 phosphatase route a MAPK cascade to multiple outcomes. *EMBO J.* **23**, 2564-2576.

Ayscough, K. R. and Drubin, D. G. (1998). A role for the yeast actin cytoskeleton in pheromone receptor clustering and signalling. *Curr. Biol.* **8**, 927-930.

Bar, E. E., Ellicott, A. T. and Stone, D. E. (2003). Gbetagamma recruits Rho1 to the site of polarized growth during mating in budding yeast. *J. Biol. Chem.* **278**, 21798-21804.

Bardwell, L. (2004). A walk-through of the yeast mating pheromone response pathway. *Peptides* **25**, 1465-1476.

Bokoch, G. M. (2003). Biology of the p21-activated kinases. *Annu. Rev. Biochem.* **72**, 743-781.

Bretscher, A. (2003). Polarized growth and organelle segregation in yeast: the tracks, motors, and receptors. *J. Cell Biol.* **160**, 811-816.

Buehrer, B. M. and Errede, B. (1997). Coordination of the mating and cell integrity mitogen-activated protein kinase pathways in Saccharomyces cerevisiae. *Mol. Cell. Biol.* **17**, 6517-6525.

Burack, W. R. and Shaw, A. S. (2000). Signal transduction: hanging on a scaffold. *Curr. Opin. Cell Biol.* **12**, 211-216.

Dohlman, H. G. and Thorner, J. W. (2001). Regulation of G protein-initiated signal transduction in yeast: paradigms and principles. *Annu. Rev. Biochem.* **70**, 703-754.

Dong, Y., Pruyne, D. and Bretscher, A. (2003). Formin-dependent actin assembly is regulated by distinct modes of Rho signaling in yeast. *J. Cell Biol.* **161**, 1081-1092.

Drgonova, J., Drgon, T., Roh, D. H. and Cabib, E. (1999). The GTP-binding protein Rho1p is required for cell cycle progression and polarization of the yeast cell. *J. Cell Biol.* **146**, 373-387.

Dustin, M. L. and Cooper, J. A. (2000). The immunological synapse and the actin cytoskeleton: molecular hardware for T cell signaling. *Nat. Immunol.* **1**, 23-29.

Elion, E. A. (1995). Ste5: a meeting place for MAP kinases and their associates. *Trends Cell Biol.* **5**, 322-327.

Elion, E. A. (2001). The Ste5p scaffold. *J. Cell Sci.* **114**, 3967-3978.

Elion, E. A., Grisafi, P. L. and Fink, G. R. (1990). FUS3 encodes a cdc2+/CDC28-related kinase required for the transition from mitosis into conjugation. *Cell* **60**, 649-664.

Elion, E. A., Brill, J. A. and Fink, G. R. (1991). FUS3 represses CLN1 and CLN2 and in concert with KSS1 promotes signal transduction. *Proc. Natl. Acad. Sci. USA* **88**, 9392-9396.

Elion, E. A., Satterberg, B. and Kranz, J. E. (1993). FUS3 phosphorylates multiple components of the mating signal transduction cascade: evidence for STE12 and FAR1. *Mol. Biol. Cell* **4**, 495-510.

Erickson, J. W. and Cerione, R. A. (2001). Multiple roles for Cdc42 in cell regulation. *Curr. Opin. Cell Biol.* **13**, 153-157.

Etienne-Manneville, S. and Hall, A. (2003). Cell polarity: Par6, a PKC and cytoskeletal crosstalk. *Curr. Opin. Cell Biol.* **15**, 67-72.

Evangelista, M., Blundell, K., Longtine, M. S., Chow, C. J., Adames, N., Pringle, J. R., Peter, M. and Boone, C. (1997). Bni1p, a yeast formin

linking cdc42p and the actin cytoskeleton during polarized morphogenesis. *Science* **276**, 118-122.

Evangelista, M., Pruyne, D., Amberg, D. C., Boone, C. and Bretscher, A. (2002). Formins direct Arp2/3-independent actin filament assembly to polarize cell growth in yeast. *Nat. Cell Biol.* **4**, 32-41.

Farley, F., Satterberg, B., Goldsmith, E. A. and Elion, E. A. (1999). Relative dependance of different outputs of the *Saccharomyces cerevisiae* pheromone response pathway on the MAP kinase Fus3. *Genetics* **151**, 1425-1444.

Garrington, T. P. and Johnson, G. L. (1999). Organization and regulation of mitogen-activated protein kinase signaling pathways. *Curr. Opin. Cell Biol.* **11**, 211-218.

Ge, L., Ly, Y., Hollenberg, M. and DeFea, K. (2003). A beta-arrestin-dependent scaffold is associated with prolonged MAPK activation in pseudopodia during protease-activated receptor-2-induced chemotaxis. *J. Biol. Chem.* **278**, 34418-34426.

Gulli, M. P. and Peter, M. (2001). Temporal and spatial regulation of Rho-type guanine-nucleotide exchange factors: the yeast perspective. *Genes Dev.* **15**, 365-379.

Henrique, D. and Schweisguth, F. (2003). Cell polarity: the ups and downs of the Par6/aPKC complex. *Curr. Opin. Genet. Dev.* **13**, 341-350.

Jaquenoud, M. and Peter, M. (2000). Gic2p may link activated Cdc42p to components involved in actin polarization, including Bni1p and Bud6p (Aip3p). *Mol. Cell. Biol.* **20**, 6244-6258.

Karpova, T. S., Reck-Peterson, S. L., Elkind, N. B., Mooseker, M. S., Novick, P. J. and Cooper, J. A. (2000). Role of actin and Myo2p in polarized secretion and growth of Saccharomyces cerevisiae. *Mol. Biol. Cell* **11**, 1727-1737.

Kelkar, N., Gupta, S., Dickens, M. and Davis, R. J. (2000). Interaction of a mitogen-activated protein kinase signaling module with the neuronal protein JIP3. *Mol. Cell. Biol.* **20**, 1030-1043.

Kohno, H., Tanaka, K., Mino, A., Umikawa, M., Imamura, H., Fujiwara, T., Fujita, Y., Hotta, K., Qadota, H. and Watanabe, T. et al. (1996). Bni1p implicated in cytoskeletal control is a putative target of Rho1p small GTP binding protein in Saccharomyces cerevisiae. *EMBO J.* **15**, 6060-6068.

Lamson, R. E., Winters, M. J. and Pryciak, P. M. (2002). Cdc42 regulation of kinase activity and signaling by the yeast p21-activated kinase Ste20. *Mol. Cell. Biol.* **22**, 2939-2951.

Leof, E. B. (2000). Growth factor receptor signalling: location, location, location. *Trends Cell Biol.* **10**, 343-348.

Lillie, S. H. and Brown, S. S. (1994). Immunofluorescence localization of the unconventional myosin, Myo2p, and the putative kinesin-related protein, Smy1p, to the same regions of polarized growth in Saccharomyces cerevisiae. *J. Cell Biol.* **125**, 825-842.

Lyons, D. M., Mahanty, S. K., Choi, K. Y., Manandhar, M. and Elion, E. A. (1996). The SH3-domain protein Bem1 coordinates mitogen-activated protein kinase cascade activation with cell cycle control in Saccharomyces cerevisiae. *Mol. Cell. Biol.* **16**, 4095-4106.

Mahanty, S. K., Wang, Y., Farley, F. W. and Elion, E. A. (1999). Nuclear shuttling of yeast scaffold Ste5 is required for its recruitment to the plasma membrane and activation of the mating MAPK cascade. *Cell* **98**, 501-512.

Maleri, S., Ge, Q., Hackett, E. A., Wang, Y., Dohlman, H. G. and Errede, B. (2004). Persistent activation by constitutive Ste7 promotes Kss1-mediated invasive growth but fails to support Fus3-dependent mating in yeast. *Mol. Cell. Biol.* **24**, 9221-9238.

Marchler-Bauer, A., Anderson, J. B., DeWeese-Scott, C., Fedorova, N. D., Geer, L. Y., He, S., Hurwitz, D. I., Jackson, J. D., Jacobs, A. R. and Lanczycki, C. J. et al. (2003). CDD: a curated Entrez database of conserved domain alignments. *Nucleic Acids Res.* **31**, 383-387.

Matheos, D., M., Metodiev, M., Muller, E., Stone, D. and Rose, M. D. (2004). Pheromone-induced polarization is dependent on the Fus3p MAPK acting through the formin Bni1p. *J. Cell Biol.* **165**, 99-109.

Morrison, D. K. and Davis, R. J. (2003). Regulation of MAP kinase signaling modules by scaffold proteins in mammals. *Annu. Rev. Cell Dev. Biol.* **19**, 91-118.

Muller, J., Ory, S., Copeland, T., Piwnica-Worms, H. and Morrison, D. K. (2001). C-TAK1 regulates Ras signaling by phosphorylating the MAPK scaffold, KSR1. *Mol. Cell* **8**, 983-993.

Ozaki-Kuroda, K., Yamamoto, Y., Nohara, H., Kinoshita, M., Fujiwara, T., Irie, K. and Takai, Y. (2001). Dynamic localization and function of Bni1p at the sites of directed growth in Saccharomyces cerevisiae. *Mol. Cell. Biol.* **21**, 827-839.

Palmieri, S. J. and Haarer, B. K. (1998). Polarity and division site specification in yeast. *Curr. Opin. Microbiol.* **1**, 678-686.

Pruyne, D. W., Schott, D. H. and Bretscher, A. (1998). Tropomyosin-containing actin cables direct the Myo2p-dependent polarized delivery of secretory vesicles in budding yeast. *J. Cell Biol.* **143**, 1931-1945.

Pryciak, P. M. and Huntress, F. A. (1998). Membrane recruitment of the kinase cascade scaffold protein Ste5 by the Gbetagamma complex underlies activation of the yeast pheromone response pathway. *Genes Dev.* **12**, 2684-2697.

Reck-Peterson, S. L., Novick, P. J. and Mooseker, M. S. (1999). The tail of a yeast class V Myosin, Myo2p, functions as a localization domain. *Mol. Biol. Cell* **10**, 1001-1017.

Sagot, I., Klee, S. K. and Pellman, D. (2002). Yeast formins regulate cell polarity by controlling the assembly of actin cables. *Nat. Cell Biol.* **4**, 42-50.

Saka, A., Abe, M., Okano, H., Minemura, M., Qadota, H., Utsugi, T., Mino, A., Tanaka, K., Takai, Y. and Ohya, Y. (2001). Complementing yeast rho1 mutation groups with distinct functional defects. *J. Biol. Chem.* **276**, 46165-46171.

Siekhaus, D. E. and Drubin, D. G. (2003). Spontaneous receptor-independent heterotrimeric G-protein signalling in an RGS mutant. *Nat. Cell Biol.* **5**, 231-235.

Sprague, G. F., Jr (1991). Assay of yeast mating reaction. *Methods Enzymol.* **194**, 77-93.

Stevenson, B. J., Rhodes, N., Errede, B. and Sprague, G. F., Jr (1992). Constitutive mutants of the protein kinase STE11 activate the yeast pheromone response pathway in the absence of the G protein. *Genes Dev.* **6**, 1293-1304.

Takenawa, T. and Miki, H. (2001). WASP and WAVE family proteins: key molecules for rapid rearrangement of cortical actin filaments and cell movement. *J. Cell Sci.* **114**, 1801-1809.

Vale, R. D. (2003). The molecular motor toolbox for intracellular transport. *Cell* **112**, 467-480.

van Drogen, F., Stucke, V. M., Jorritsma, G. and Peter, M. (2001). MAP kinase dynamics in response to pheromones in budding yeast. *Nat. Cell Biol.* **3**, 1051-1059.

Verhey, K. J., Meyer, D., Deehan, R., Blenis, J., Schnapp, B. J., Rapoport, T. A. and Margolis, B. (2001). Cargo of kinesin identified as JIP scaffolding proteins and associated signaling molecules. *J. Cell Biol.* **152**, 959-970.

Wang, Y., Chen, W., Simpson, D. M. and Elion, E. A. (2005). Cdc24 regulates nuclear shuttling and recruitment of the Ste5 scaffold to a heterotrimeric G protein in S. cerevisiae. *J. Biol. Chem.* **280**, 13084-13096.

Yamochi, W., Tanaka, K., Nonaka, H., Maeda, A., Musha, T. and Takai, Y. (1994). Growth site localization of Rho1 small GTP-binding protein and its involvement in bud formation in Saccharomyces cerevisiae. *J. Cell Biol.* **125**, 1077-1093.

Zarzov, P., Mazzoni, C. and Mann, C. (1996). The SLT2 (MPK1) MAP kinase is activated during periods of polarized cell growth in yeast. *EMBO J.* **15**, 83-91.

Zhao, Z. S., Leung, T., Manser, E. and Lim, L. (1995). Pheromone signalling in *Saccharomyces cerevisiae* requires the small GTP-binding protein Cdc42p and its activator Cdc24. *Mol. Cell. Biol.* **15**, 5246-5257.

Zigmond, S. H. (2004). Formin-induced nucleation of actin filaments. *Curr. Opin. Cell Biol.* **16**, 99-105.

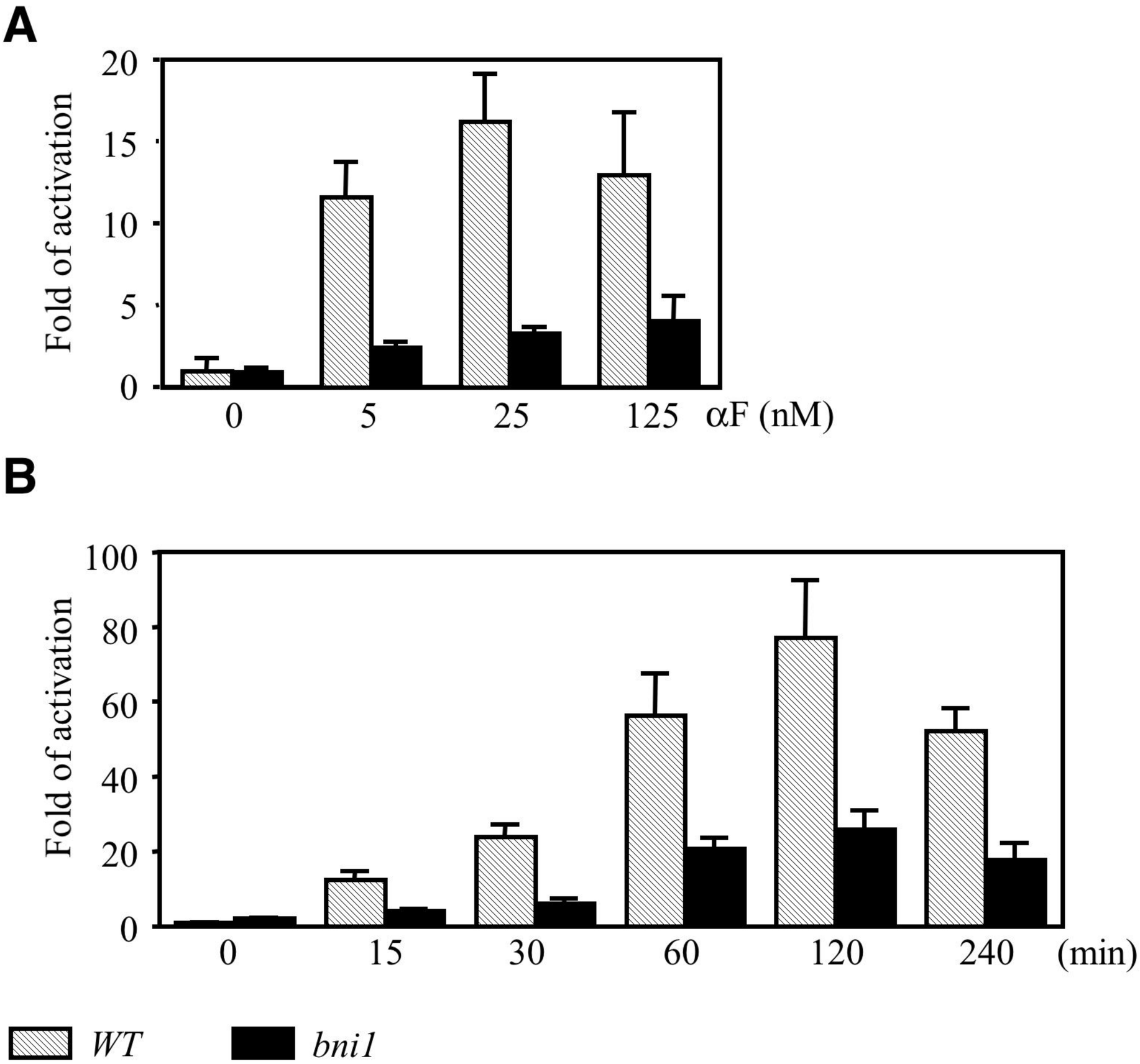

Fig. S1. *bni1* deletion reduces mating MAPK activation

Fus3 kinase activity in the experiments shown in Fig. 2A and 2B was quantified. Films were scanned and bands were analyzed with Scion Image software. The entire lane (including bands of both endogenous and exogenous substrates) of individual kinase assays was quantified and normalized to the level of Fus3 protein. Relative values (wild type before treatment was set to 1) are shown. (A) Dose response; (B) Time course. Values represent average ± STD of two independent experiments.

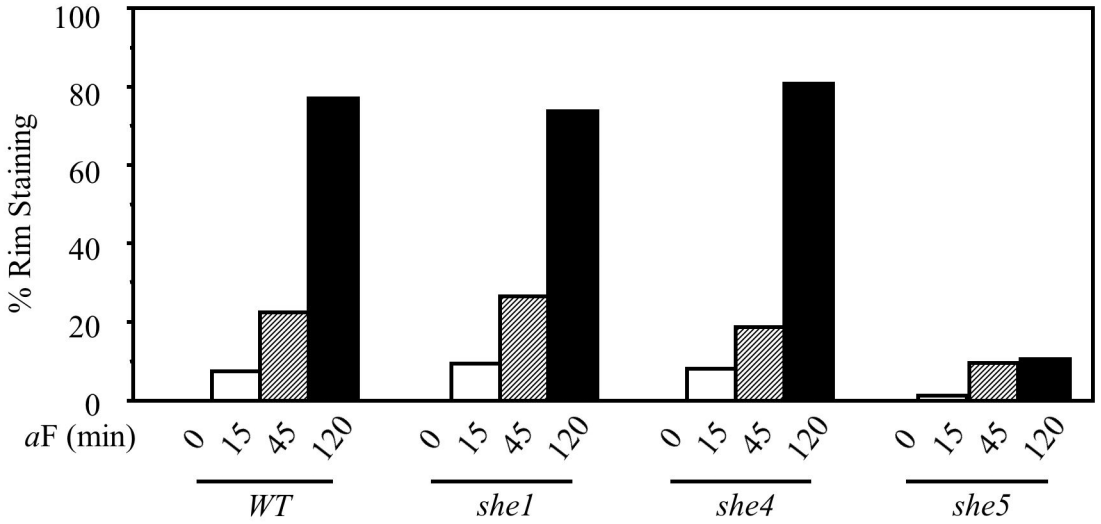

Fig. S2. Ste5 recruitment in *she* mutants

WT (EYL1684), *she1*(EYL1685), *she4* (EYL1688) and *she5* (EYL1689) cells expressing Ste5-Myc9 (EBL453) were treated with 5 μM α factor for 0, 15, 45, and 120 minutes. Indirect immunofluorescence was done to detect Ste5-Myc as in Fig. 3B.

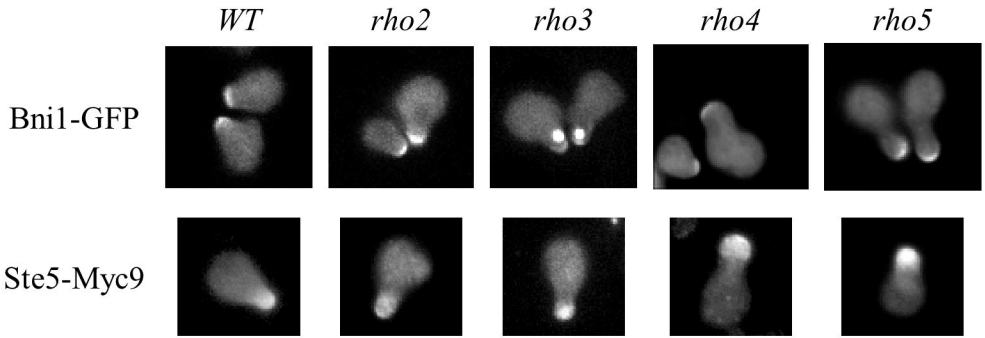

Fig. S3. Bni1-GFP and Ste5-Myc9 recruitment in *rho2~5* mutants
WT, rho2, rho3, rho4 and *rho5* null mutant cells expressing Bni1-GFP or Ste5-Myc9 were treated with 5 μM α factor for 2 hours. Bni1-GFP was visualized by direct fluorescence microscopy and Ste5-Myc9 was visualized by indirect immunofluorescence.

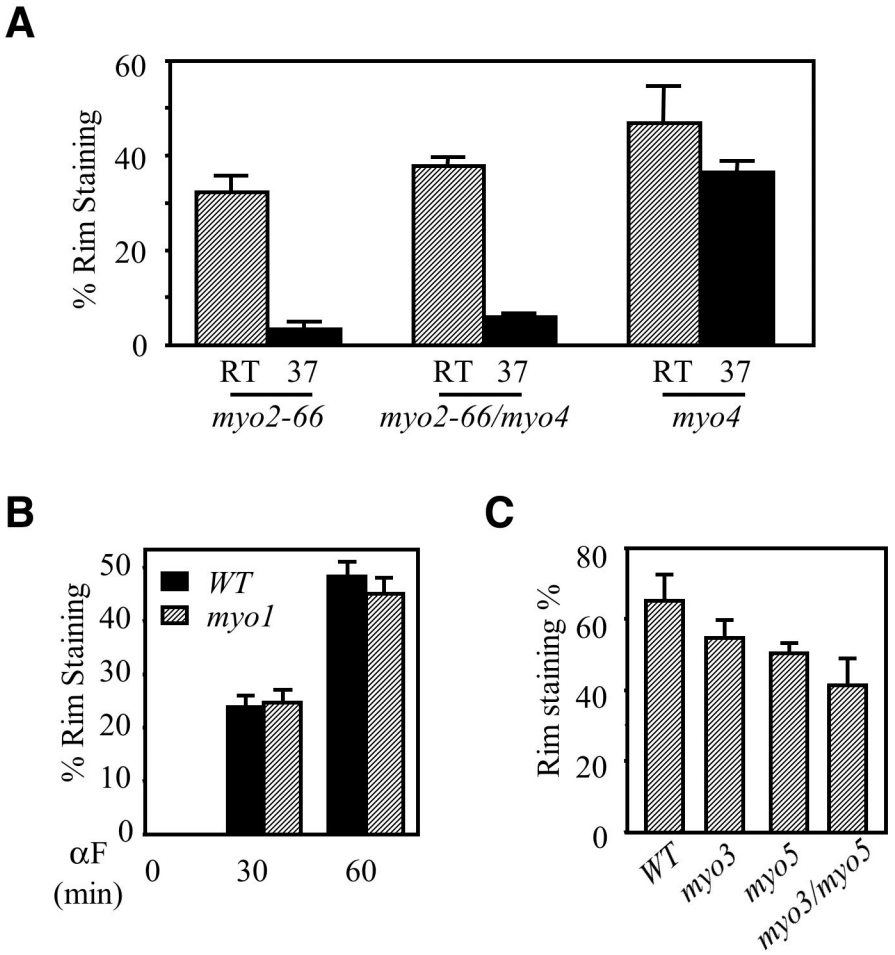

Fig. S4. Ste5-Myc9 recruitment in *myo* mutants

(A) Ste5-Myc9 localization *myo2-66/myo4* cells. TAgNLSK128TSte5-Myc9 was expressed in *myo2-66* (QMY630), *myo4* (QMY631) and *myo2-66/myo4* (QMY632) strains. The cells were treated as in (Fig. 7A).

(B) Ste5 localization in *myo1* mutants. *WT* (EY699) and *myo1* (EYL1098) cells expressing Ste5-Myc9 (EYL453) were treated with 5 μM α factor for 30 and 60 minutes, then fixed and treated for indirect immunofluorescence to observe Ste5-Myc9. Ste5-Myc9 rim staining was tallied in over 300 cells.

(C) Ste5-Myc9 recruitment in *myo3* and *myo5* mutants. *WT* (QMY550), *myo3D* (QMY483), *myo5*(QMY484), *or myo3/myo5* (QMY485) cells expressing Ste5-Myc9 (EBL453) were treated with 5 μM α factor for 60 minutes.

Accepted 5 April 2005
Journal of Cell Science 118, 2837-2848 Published by The Company of Biologists 2005
doi:10.1242/jcs.02418

Supplementary material

Yeast strains

Strains were grown in rich medium or synthetic medium as described (Guthrie and Fink, 1991).

Table S1. Yeast strains

Strains	Genotype	Source
EY492	*MATα ura3-1 leu2-3,112 trp1-1 his3-11 ade2-1 can1-100 Gal*$^+$	R. Rothstein
EY699	*ura3-1 leu2-3,112 trp1-1 his3-11 ade2-1 can1-100 Gal*$^+$	R. Rothstein
EY700	EY699 *fus3-6::LEU2*	E. Elion
EY957	EY699 *sst1*	E. Elion
EY1775	EY957 *ste5::TRP3*	E. Elion
EYL300	*MATa leu2-3 ura3-52*	R. Li
EYL302	*MATa leu2-3 ura3-52 cdc42-1*	R. Li
EYL427	*bni1::KAN ura3-1 leu2-3,112 trp1-1 his3-11 ade2-100 ade3*	D. Pellman
EYL428	*bni1::KAN ura3-1 leu2-3,112 trp1-1 his3-11 ade2-100 ade3 MATα*	D. Pellman
EYL917	EYL427 *sst1*	B.N. Lee
EYL1096	*sst1::LEU2 FUS3GFP::HIS3 ura3-1 leu3-3,112 trp1-1 his3-11 ade2-1 can1-100*	A. Levchenko
EYL1098	*myo1::KAN ura3-1 leu2-3,112 trp1-1 his3-11 ade2-1 can1-100 Gal*$^+$	R. Li
EYL1730	*bnr1::KAN ura3-1 leu2-3,112 trp1-1 his3-11 ade2-100*	D. Pellman
EYL1735	*tpm1-2::LEU2 tpm2::HIS3 his3Δ-200 leu2-3,112 lys2-801 trp1-1 ura3-52*	A. Bretscher
EYL1736	*tpm2::HIS3 his3Δ-200 leu2-3,112 lys2-801 trp1-1 ura3-52*	A. Bretscher
EYL1748	*bni1::BNI1#1::HIS3 bnr1::KAN ura3-1 leu2-3,112 trp1-1 his3-11 ade2-100*	D. Pellman
EYL1765	*his3Δ1 leu2Δ0 met15Δ0 ura3Δ0*	Res Gene
EYL1802	*MATα MYO2::HIS3 his3-Δ200 ura3-52 leu2-3,112 lys2-801 ade2-101 Gal*$^+$	D. Pellman
EYL1807	*MATα myo2-66::HIS3 his3-Δ200 ura3-52 leu2-3,112 lys2-801 ade2-101 Gal*$^+$	D. Pellman
QMY27	*sst1::LEU2 bni1::kanR FUS3GFP::HIS3 ura3-1 leu3-3,112 trp1-1 his3-11 ade2-1* c*an1-100*	This study
QMY458	EYL1802 switched to *MATa*	This study
QMY459	EYL1807 switched to *MATa*	This study

QMY483	*myo3::HIS3 ura3 leu2 trp1 his3 ade2*	R. Li
QMY484	*myo5::TRP1 ura3 leu2 trp1 his3 ade2*	R. Li
QMY485	*myo3::HIS myo5::TRP1 ura3 leu2 trp1 his3 ade2*	R. Li
QMY550	*ura3 leu2 trp1 his3 ade2*	R. Li
QMY551	*rho1-104 ura3 leu2 trp1 his3 ade2*	R. Li
QMY553	*rho1::HIS3 rho1-2 LEU2 ura3 leu2 trp1 his3 ade2*	R. Li
QMY574	*rho3::KAN his3Δ1 leu2Δ0 met15Δ0 ura3Δ0*	This study
QMY576	*rho5::KAN his3Δ1 leu2Δ0 met15Δ0 ura3Δ0*	This study
QMY630	*myo2-66::HIS3*	This study
QMY631	*myo4::KAN*	This study
QMY632	*myo2-66::HIS3 myo4::KAN*	This study
5126	*rho4::KAN his3Δ1 leu2Δ0 met15Δ0 ura3Δ0*	Res Gene
7230	*rho2::KAN his3Δ1 leu2Δ0 met15Δ0 ura3Δ0*	Res Gene
22032	*MATa rho5::KAN his3Δ1 leu2Δ0 met15Δ0 ura3Δ0*	Res Gene
	MATα rho5::KAN his3Δ1 leu2Δ0 met15Δ0 ura3Δ0	
22277	*MATa rho3::KAN his3Δ1 leu2Δ0 met15Δ0 ura3Δ0*	Res Gene
	MATα rho3::KAN his3Δ1 leu2Δ0 met15Δ0 ura3Δ0	

All strains except EY492, EYL428, 22032 and 22277 are *MATa*.

QMY27 was produced by cross of EYL428 with EYL1096. QMY630-632 were created by crossing EYL1685 with EYL1807 (*she1* is *myo4*). QMY574 and QMY576 were made by sporulation of 22277 and 22032.

Plasmid construction

All *BNI1* plasmids were made from a pRS316-based vector (PB1025, former name p182, see Evangelista et al., 1997) containing the *BNI1* coding sequence with 800 base pairs (bp) upstream and 1600 bp downstream sequence. The Rho-binding domain deletion mutant, *bni1ΔRBD* (QMB16, deletes aa 90-343), was made from two PCR amplified fragments of *BNI1* using the following primers: -788~268 fragment: 5′-ACGCGGATCCTTCACCGCTTTCGCACCTACTT-3′(*Bam*HI site at 5′ terminus), 5′-TCCCCGCGGCGATTTTTTATTCAACGGCCT-3′ (*Sac*II site at 3′ terminus) and 1031~2472 fragment: 5′-CTACCGCGGCGAATCCTGGCAGACAAACTT-3′ (*Sac*II site at 5′ terminus), 5′-TGCATGTCTCGAGTTCATACCTCTGGTGCCTTC-3′. The PCR products were cut with *Bam*HI/*Sac*II and *Sac*II/*Xho*I respectively, then performed a 3-way ligation with *Bam*HI/*Xho*I vector fragment of PB1025 to produce QMB16. The *Bam*HI/*Xho*I fragment of QMB16 containing *bni1ΔRBD* mutation was inserted into EBL334 to produce QMB79 (*bni1ΔRBD-GFP)*. The *bni1ΔFH1FH2* mutant (QBM5, deletes

aa 1230-1748) was made by cloning the *BNI1* gene into *Bam*HI-*Eag*I sites of pBR322 to make QMB3. A *BNI1* fragment from the *Xho*I site to the FH1 domain (nucleotides 3572-4791) was PCR amplified with primers: 5′GAACTCGAGCCTA AATTCTTCAG-3′ and 5′-AGATCCGCGGCAGTAGAGAGATCTTCTGCG-3′ (*Sac*II site at 5′ terminus). This PCR product was used to replace the *Xho*I~*Sac*II fragment of *BNI1* gene in QMB3 to make QMB4. Then the *Bam*HI-*Eag*I fragment of QMB4 was cloned into pRS316 to make QMB5. To make *bni1ΔFH1* (QMB21, deletes aa 1230-1328), fragment from *Xho*I site to FH1 domain (3572-4791) was PCR amplified by the same way as for FH domain deletion, but added a *Sph*I site instead of *Sac*II site to the second primers: 5′-GATGCATGCAGTAGAGAGAT CTTCTGCG-3′. Fragment from the end of FH1 to *Sac*II site (5086-6352) were PCR amplified with 5′ primer: 5′-CATGCATGCGCATCGCAAATCAAATCAGCT-3′ (*Sph*I site at 5′ terminus) and 3′ primer: 5′-CTTCCGCGGCTAGATTTTGCGCTT-3′. The first and second PCR products were digested with *Xho*I/*Sph*I and S*ph*I/*Sac*II respectively, then used in a 3-way ligation with the *Xho*I/*Sac*II fragment of QMB3 to make QMB19. The *Bam*HI~*Eag*I fragments of QMB19 was cloned into pRS316 to make QMB21. The same strategy was used to make *bni1ΔFH2* (QMB22, deletes aa 1492-1640), except a different 3′ primer (5′-TGTAGCATGCCCTCACGCC CTCCCAGTCTG-3′) for the first PCR, which amplifies fragment from *Xho*I site to FH2 domain (3572-5577), and a different 5′ primers (5′-CGATGCATGCTCCATTGAGCAGTTAGTTAA-3′) for the second PCR, which amplifies fragment from the end of FH2 domain to *Sac*II site (6021-6352). QMB34 (*bni1ΔCT,* deletes aa 1749-1953) was made by cloning *Bam*HI-*Eag*I fragment of PB1046 (Lee et al., 1999) into pRS315.

Table S2. Plasmids used in this study

Plasmids	Description			Source
QMB5	*bni1ΔFH1FH2*	*CEN*	*URA3*	This study
QMB16	*bni1ΔRBD*	*CEN*	*URA3*	This study
QMB21	*bni1ΔFH1*	*CEN*	*URA3*	This study
QMB22	*bni1ΔFH2*	*CEN*	*URA3*	This study
QMB34	*bni1ΔCT*	*CEN*	*LEU2*	This study
QMB75	*MYO2DN*	*GAL1*	*LEU2*	S. Reck-Peterson
QMB79	*bni1ΔRBD-GFP*	*CEN(ADH1)*	*URA3*	This study
QMB80	*MYO2-HA*	*CEN*	*HIS3*	L. Weisman
EBL95	*FUS1-LACZ*	*2*	*LEU2*	Elion *et al.* (1990)
EBL204	*STE5-CTM*	*CEN(GAL1)*	*LEU2*	Pryciak *et al.* (1998)

EBL284	*STE11-4*	*CEN*	*HIS3*	H. Madhani
EBL332	*BNI1-HA4*	*CEN*	*URA3*	D. Pellman
EBL334	*BNI1-GFP*	*CEN(ADH1)*	*URA3*	D. Pellman
EBL358	*STE5-MYC9*	*CEN*	*URA3*	Mahanty *et al.* (1999)
EBL365	*STE5-MYC9*	*2*	*URA3*	Mahanty *et al.* (1999)
EBL367	*STE5-GFP*	*CEN(CUP1)*	*URA3*	Mahanty *et al.* (1999)
EBL444	*TAgNLS^{K128T}-STE5-M9*	*2*	*URA3*	Mahanty *et al.* (1999)
EBL453	*STE5-MYC9*	*2*	*LEU2*	Mahanty *et al.* (1999)
EBL511	*GFP-STE20*	*CEN*	*URA3*	Leberer *et al.* (1997)
EBL664	*GFP-CDC24*	*CEN(MET)*	*LEU2*	Toenjes *et al.* (1999)
PYEE1102	*FUS3-HA*	*CEN*	*HIS3*	Elion *et al.* (1993)

Supplemental References

Elion, E.A., Grisafi, P.L. and Fink, G.R. (1990). FUS3 encodes a cdc2+/CDC28-related kinase required for the transition from mitosis into conjugation. *Cell.* **60,** 649-664.

Guthrie, C. and Fink, G.R. (1991). Guide to yeast genetics and molecular biology. *Methods Enzymol.* **194,** 1-933.

Lee, L., Klee, S.K., Evangelista, M., Boone, C. and Pellman, D. (1999). Control of mitotic spindle position by the Saccharomyces cerevisiae formin Bni1p. *J. Cell Biol.* **144,** 947-961.